Amphiphilic AIEgen-polymer aggregates: Design, self-assembly and biomedical applications

Received: 12 August 2021 | Revised: 13 September 2021 | Accepted: 26 September 2021

DOI: 10.1002/agt2.128

Aggregate Open Access WILEY

REVIEW

Amphiphilic AIEgen-polymer aggregates: Design, self-assembly and biomedical applications

Shoupeng Cao | **Jingxin Shao** | **Loai K. E. A. Abdelmohsen** | **Jan C. M. van Hest**

Bio-Organic Chemistry, Institute for Complex Molecular Systems, Eindhoven University of Technology, Eindhoven, The Netherlands

Correspondence
Loai K. E. A. Abdelmohsen and Jan C. M. van Hest, Bio-Organic Chemistry, Institute for Complex Molecular Systems, Eindhoven University of Technology, P.O. Box 513 (STO 3.41), 5600 MB Eindhoven, The Netherlands.
Emails: l.k.e.a.abdelmohsen@tue.nl; j.c.m.v.hest@tue.nl

Funding information
ERC Advanced Grant Artisym, Grant/Award Number: 694120; Dutch Ministry of Education, Culture and Science, Grant/Award Number: 024.001.035; NWO-NSFC Advanced Materials, Grant/Award Number: 792.001.015; European Union's Horizon 2020; Marie Sklodowska-Curie Innovative Training Networks Nanomed, Grant/Award Number: 676137; H2020 Marie Skłodowska-Curie Actions, Grant/Award Numbers: Innovative Training Networks Nanomed, (No., 676137; H2020 European Research Council, Grant/Award Number: ERC Advanced Grant Artisym 694120

Abstract
Aggregation-induced emission (AIE) is a phenomenon in which fluorescence is enhanced rather than quenched upon molecular assembly. AIE fluorogens (AIEgens) are flexible, conjugated systems that are limited in their dynamics when assembled, which improves their fluorescent properties. This intriguing feature has been incorporated in many different molecular assemblies and has been extended to nanoparticles composed of amphiphilic polymer building blocks. The integration of the fascinating AIE design principle with versatile polymer chemistry opens up new frontiers to approach and solve intrinsic obstacles of conventional fluorescent materials in nanoscience, including the aggregation-caused quenching effect. Furthermore, this integration has drawn significant attention from the nanomedicine community, due to the additional advantages of nanoparticles comprising AIEgenic molecules, such as emission brightness and fluorescence stability. In this regard, a range of AIEgenic amphiphilic polymers have been developed, displaying enhanced emission in the self-assembly/aggregated state. AIEgenic assemblies are regarded as attractive nanomaterials with inherent fluorescence, which display promising features in a biomedical context, for instance in biosensing, cell/tissue imaging and tracking, as well as (photo) therapeutics. In this review, we describe recent strategies for the design and synthesis of novel types of AIEgenic amphiphilic polymers via facile approaches including direct conjugation to natural/synthetic polymers, polymerization, post-polymerization and supramolecular host−guest interactions. Their self-assembly behavior and biomedical potential will be discussed.

KEYWORDS
aggregation-induced emission, amphiphilic polymers, biomedical applications, nanomotors, supramolecular self-assembly

1 | INTRODUCTION

The incorporation of fluorescent properties in nanoparticles is useful for a wide variety of biological applications, such as in vivo tracking, monitoring bio-distribution and cell/tissue imaging.[1–3] Traditionally, fluorescence is introduced by utilizing conventional dyes, such as porphyrins, boron dipyrromethene (BODIPY), fluorescein isothiocyanate (FITC) and cyanine imaging agents.[4–6] Whilst frequently used, these conventional luminogens however are recognized to suffer from several drawbacks. Dye leakage is often observed for non-covalently functionalized particles, although this can be solved by chemical conjugation.[7–8] Bleaching is also often encountered, which is a more fundamental problem and makes it difficult to precisely track the particles for prolonged periods.[9] In addition, the emissive moieties after self-assembly or physical encapsulation in the nanoparticles have a strong tendency to aggregate together, because of the hydrophobic interactions and intensive π-π stacking, resulting in the formation of H-type aggregates.[10] This in turn strongly quenches their emission, resulting in the aggregation-caused quenching (ACQ) effect.[11–12] Only in the case that the embedded luminogens are isolated, these dyes become intensely fluorescent. This is often only possible upon release of the fluorophores or dissociation of the particles.[13] However, this makes it difficult to track and collect the information of the initial nanoparticles, as well as to evaluate their bio-distribution profile in a precise manner. Generally, additional chemistry is required to prevent the ACQ effect of functional luminogens. This is especially

relevant when the photochemical features are exploited in a therapeutic setting, as for example is the case with photodynamic therapy (PDT).[14–16] Here, upon irradiation, the excited fluorophores can transfer their energy to oxygen, creating reactive singlet oxygen species (ROS). The ACQ effect strongly diminishes the therapeutic efficacy of this process and therefore needs to be omitted. For instance, to reduce the ACQ effect of porphyrin moieties and achieve a satisfying therapeutic performance, Zhang et al. installed a polyhedral oligomeric silsesquioxane unit on the backbone of porphyrin-based amphiphilic polymers in an alternating fashion.[17] This provided a steric effect that inhibited the π-π stacking of the functional photosensitizer, providing a strategy to enhance the PDT efficacy.

A strategy that circumvents the abovementioned drawbacks in a facile manner is to incorporate a special class of luminogens with the feature of aggregation-induced emission (AIEgen) into the polymer building blocks.[18–21] Generally, AIEgenic molecules are dynamic structures with rotor-like features, which transfer the excitation energy after activation via non-radiative decay in the molecular state.[22–24] Thus, AIEgenic compounds are typically non-emissive in the molecular state, for example, when solubilized in solvents like dimethyl sulfoxide (DMSO) and tetrahydrofuran (THF).[18] Upon aggregation or assembly, restriction of rotation leads to a reduced non-radiative energy dissipation of the AIEgenic molecules, resulting in a bright and stable emission.[25] In addition, the close intermolecular π-π stacking interactions are also reduced because of the non-planar molecular structure of the AIE molecules, which contributes to a further increase in emission intensity.[26] In this case, the AIE compounds exhibit high emission efficiency when a high concentration of AIE molecules is aggregated, due to the restriction of the intramolecular motion effect. In addition, compared to ACQ fluorophores, AIE emission produces less heat, due to the reduced non-radiative energy dissipation. This makes them more resistant to photobleaching than a single fluorophore molecule (e.g., in the ACQ dyes).[27–28] Combined with their anti-photo-bleaching capacity, the excellent optical properties of AIEgenic compounds make them an ideal candidate to be used in the construction of functional nanomaterials that can be used in different fields such as fluorescent sensors, emissive probes, bioimaging and therapeutic applications.[29–32] To ensure the functional AIEgenic aggregates can be applied in a biomedical setting in the desired way, several requirements need to be fulfilled, for instance, biological safety, stability under physiological conditions, biocompatibility and biodegradability.[3,33–34] A wide range of AIEgenic nanoparticles have been constructed that optimally benefit from the intrinsic fluorescence and that show biomedical potential.[35–37]

In recent years, AIEgenic molecules have been incorporated into amphiphilic polymers, which have been used as building blocks for assembly into nanoparticles.[37–43] The versatile nature of polymer chemistry has enabled the robust incorporation of AIEgens in a range of manners to afford various functional polymeric architectures.[44–47] AIEgenic moieties are usually utilized as hydrophobic moieties, which can be conjugated to natural/synthetic hydrophilic polymers; they are also incorporated in the hydrophobic domain of amphiphilic block copolymers or tagged to the hydrophobic chain end.[39,48–50] The incorporation of AIEgens into amphiphilic polymers can also be realized by non-covalent supramolecular host-guest interactions.[51–53] AIEgenic amphiphilic polymers, upon self-assembly in an aqueous medium, yield nanosized, bright fluorescent nanoparticles. Their intrinsic fluorescence and tuneable emission allow AIEgenic aggregates to be widely used in tracking and imaging of many biological events, from in vivo biodistribution and cellular internalization, to drug release.[54–56] Their intrinsic fluorescence is furthermore also employed more actively in therapeutic modalities such as PDT and photothermal therapy (PTT).[57–60]

In addition, the chemical versatility of block copolymers in combination with the potent AIEgenic technology allows much freedom in molecular design.[61–64] This enables the creation of tailor-made AIEgenic aggregates, with control over their physicochemical properties in a facile manner, concerning size, shape, morphology, flexibility, surface chemistry (for instance charge and site-targeting ligands) and stability (including both disassembly kinetics and stimuli-responsive pathways).[65–70] Co-assembly strategies increase the variety in AIEgenic assemblies even further.[25] In this review, we mainly cover the topic of amphiphilic polymeric self-assemblies with AIE properties and summarize the recent progress in their design, synthesis, self-assembly, fluorescent behavior and biomedical applications. Rather than being comprehensive, we have limited ourselves to amphiphilic AIEgenic polymeric systems in which the AIEgen has become an integral part of the polymer building blocks; fully conjugated polymers or physical entrapment of AIEgens in polymer particles are beyond the scope of this review. We will start with highlighting the current progress of engineering novel types of AIEgenic amphiphilic polymers, illustrate it with selected examples (Figure 1) and end with a perspective on how AIE and amphiphilic polymers could be merged synergistically for a new generation of functional particles in nanomedicine.

2 | CONSTRUCTION OF AMPHIPHILIC POLYMER-BASED AIEGENIC AGGREGATES

AIEgenic molecules are chemically versatile moieties that offer many sites for modification.[20,41–42] In this regard, a range of different strategies have been developed to prepare amphiphilic polymers bearing AIE moieties. In this section, we highlight current approaches for the fabrication of amphiphilic polymers to which AIEgens are attached. We will first describe strategies in which the AIEgens are chemically conjugated to the polymers. Subsequently, we will discuss supramolecular designs. In the final part of this section, we will focus on how these building blocks are assembled into well-defined nanoparticles.

2.1 | Synthesis of AIEgenic polymeric amphiphiles

A common approach to prepare amphiphilic AIEgenic polymers is by directly conjugating them to hydrophilic synthetic polymers or natural polymers such as polysaccharides.[38,42,71] Polysaccharides are well-known for their involvement in a wide range of biological

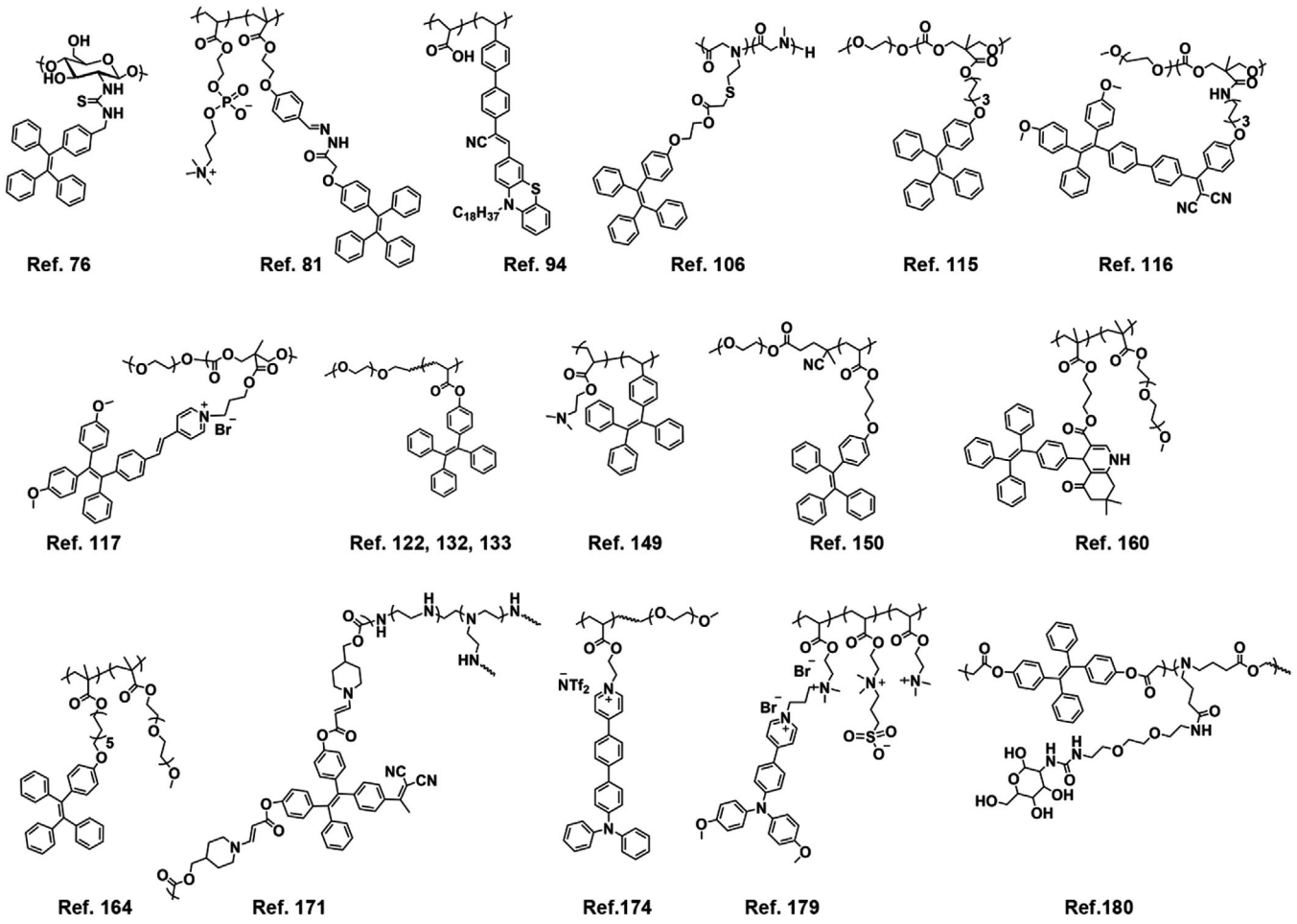

FIGURE 1 Typical design and chemical structures of different amphiphilic AIEgenic polymers

processes; they also display accessible functional moieties, which make them ideal candidates for modification reactions with AIEgens to create biocompatible/biodegradable polymeric nanoparticles with diverse architectures, reactivity and functions.[72–75] For instance, Tang et al. synthesized a polymeric fluorogenic probe by attaching a large number of tetraphenylethene (TPE) moieties to chitosan (CS).[76] This was achieved via the efficient ITC-amino chemistry, which allowed a high degree of labelling (Figure 2A). A flexible methylene spacer was inserted between the TPE phenyl ring and the ITC group. This rendered the ITC tagged TPE with higher activity, as compared to the conventionally used FITC, which allowed for more TPE labels per CS chain. Furthermore, it decoupled the AIEgen from the polymer backbone, which prevented any detrimental effects caused by possible electronic interactions and steric hindrance on the spectral features of the AIEgen. The TPE-ITC compound displayed strong emission in its solid or aggregated state in solution (Figure 2B). Unlike conventional FITC-conjugated CS (of which the emission is quenched upon increasing degrees of labelling due to the ACQ effect), the TPE-CS conjugate displayed a boosted emission as a consequence of the unique AIE effect (Figure 2C). The solubility of such TPE−CS conjugates in aqueous medium was very low, resulting in aggregates that displayed high fluorescence levels.

Besides the efficient ITC-amino chemistry that has been widely used in the preparation of functional AIEgenic materials, condensation reactions between carboxylic groups and amino/hydroxyl moieties,[77–78] Schiff base,[79] hydrazone[80–81] and various "click chemistry" methods[82–83] have also been employed as facile and robust approaches to functionalize natural/synthetic polymers with hydrophobic AIE moieties. These approaches do not only allow conjugation of AIE groups in a controlled manner, but also enable the engineering of stimuli-responsive aggregates that change their properties upon exposure to external triggers such as pH, temperature and enzyme-mediated hydrolysis.[84–86] An interesting example is the pH-sensitive zwitterionic copolymer bearing AIE active TPE moieties reported by Jin et al. (Figure 2D).[81] This polymer was prepared in two steps: The first step was the synthesis of poly(2-methacryloyloxyethyl phosphorylcholine-*co*-2-(4-formylphenoxy) ethyl methacrylate) (poly(MPC-*co*-FPEMA)) via reversible addition-fragmentation chain-transfer (RAFT) polymerization, followed by conjugating TPE to poly(MPC-*co*-FPEMA) via acid-cleavable hydrazone bonds. The assembly of these copolymers was realized via a dialysis method, in which the Milli-Q water was dropwise added to the polymer dissolved in THF and DMSO. After extensive dialysis to remove the organic solvents, the resulting spherical polymeric micelles with an average size ~200 nm were capable of being effectively loaded with hydrophobic drugs through hydrophobic and π-π interactions.[32,87–88] Combining the non-fouling properties of the zwitterionic surface, AIE active imaging and pH responsiveness, the prepared spherical polymeric

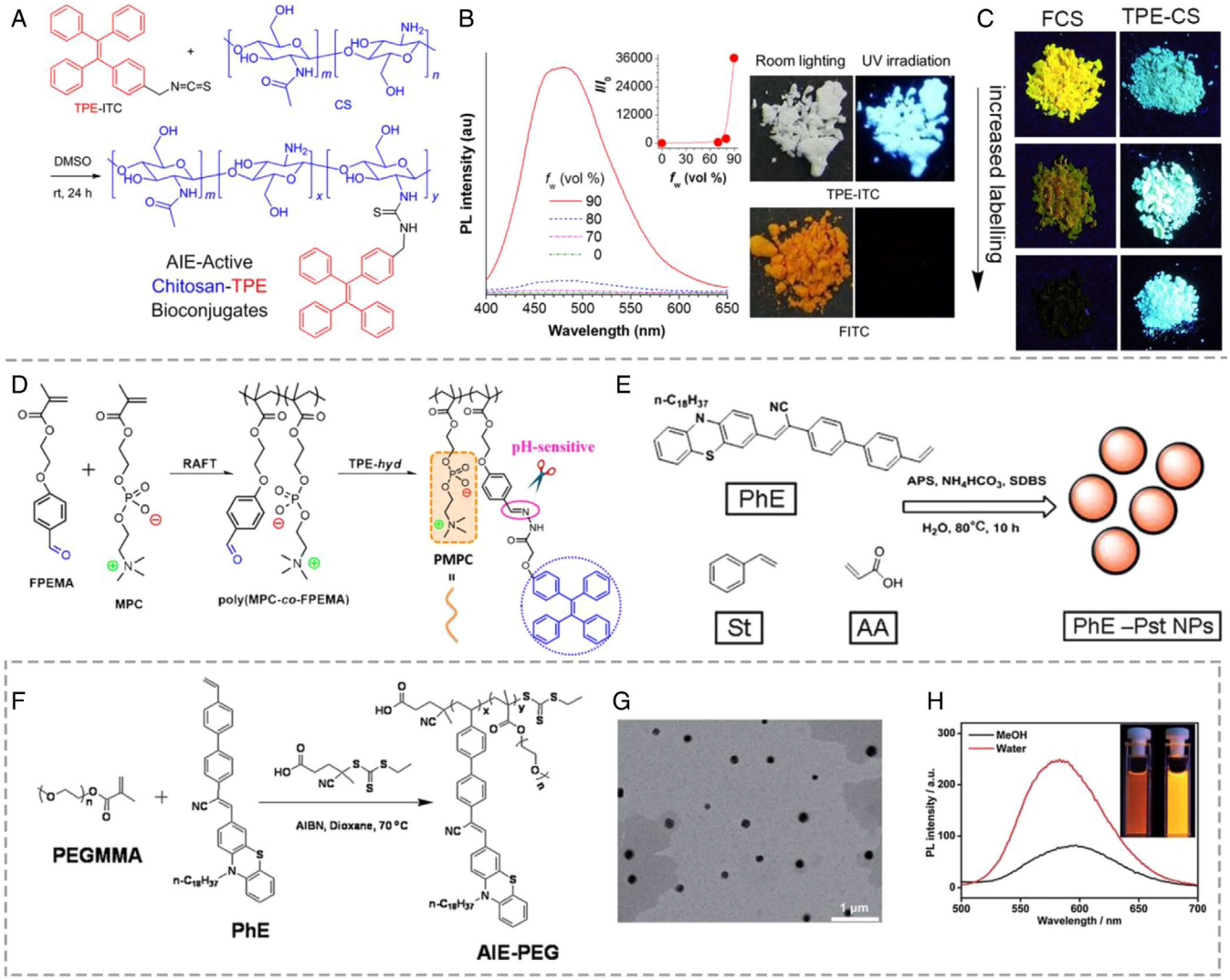

FIGURE 2 (A) Synthetic scheme towards aggregation-induced emission (AIE)-active chitosan-based bio-conjugates via isothiocyanate-amino chemistry. (B) The building block tetraphenylethene (TPE)-ITC, used for bio-conjugation, displays typical AIE features, as it is not emissive in the dissolved state, in tetrahydrofuran (THF), and increases its emission intensity with the increasing amounts of water. This is in contrast to the conventional fluorogen fluorescein isothiocyanate (FITC) which is quenched in the solid-state. (C) With increased labelling of chitosan with FITC or TPE-ITC, FITC labelling displays diminished emission, whereas the AIEgenic TPE conjugates display enhanced emission because of a further restricted intramolecular rotation. Reproduced from Ref. [76] with permission, Copyright 2013, American Chemical Society. (D) Synthetic scheme of poly(MPC-co-FPEMA) via a reversible addition-fragmentation chain-transfer (RAFT) polymerization approach, which allows post-polymerization with a TPE unit to generate AIEgenic particles with pH-responsiveness. Reproduced from Ref. [81] with permission: Copyright 2016, American Chemical Society. (E) Schematic showing the preparation of AIEgenic nanoparticles via an emulsion polymerization, which results in fluorescent particles. Reproduced from Ref. [94] with permission, Copyright 2016, the Royal Society of Chemistry. (F-H) Synthesis of amphiphilic polymers with AIEgenic monomers via RAFT polymerization, which self-assemble into spherical particles that display enhanced emission in aqueous medium compared to methanol. Reproduced from Ref. [95] with permission, Copyright 2016, the Royal Society of Chemistry

nanoparticles displayed capacity for tracking and controlled drug release in a tumour microenvironment.

Besides the abovementioned post-polymerization modification reactions, copolymerization of AIEgenic monomers can also be employed to incorporate this functionality into polymer structures. The recent advances in a number of controlled polymerization approaches allow the preparation of tailored and precise amphiphilic copolymers with controlled molecular weight, polydispersity index (Đ) and well-defined compositions.[89–93] Polymerization of an AIE active monomer into a hydrophobic block has become an attractive strategy to embed AIEgens in the polymer structure to generate well-defined AIEgenic amphiphilic polymers.[38,41–42] Radical copolymerization can easily be achieved with vinyl group-tagged AIEgenic monomers.[39] For example, Wen et al. have developed an effective strategy to prepare AIEgenic nanoparticles via emulsion polymerization, through one-step copolymerization of an AIE monomer with styrene and acrylic acid in the presence of a surfactant (sodium dodecyl sulfate) and initiator (ammonium persulfate) in an aqueous solution (Figure 2E).[94] The resultant amphiphilic AIEgenic polymers spontaneously self-assembled into ca. 200 nm spherical particles after polymerization due to hydrophobic interactions; such nanoparticles displayed uniform morphology, high water dispersibility and excellent biocompatibility. Besides, the presence of carboxyl groups also allowed for further surface modification. The same research group reported another synthesis route based on RAFT polymerization of an AIEgenic monomer with poly(ethylene glycol monomethacrylate) (PEGMMA) (Figure 2F).[95] This yielded AIEgenic amphiphilic block-polymers with well-controlled macromolecular weight (M_n)

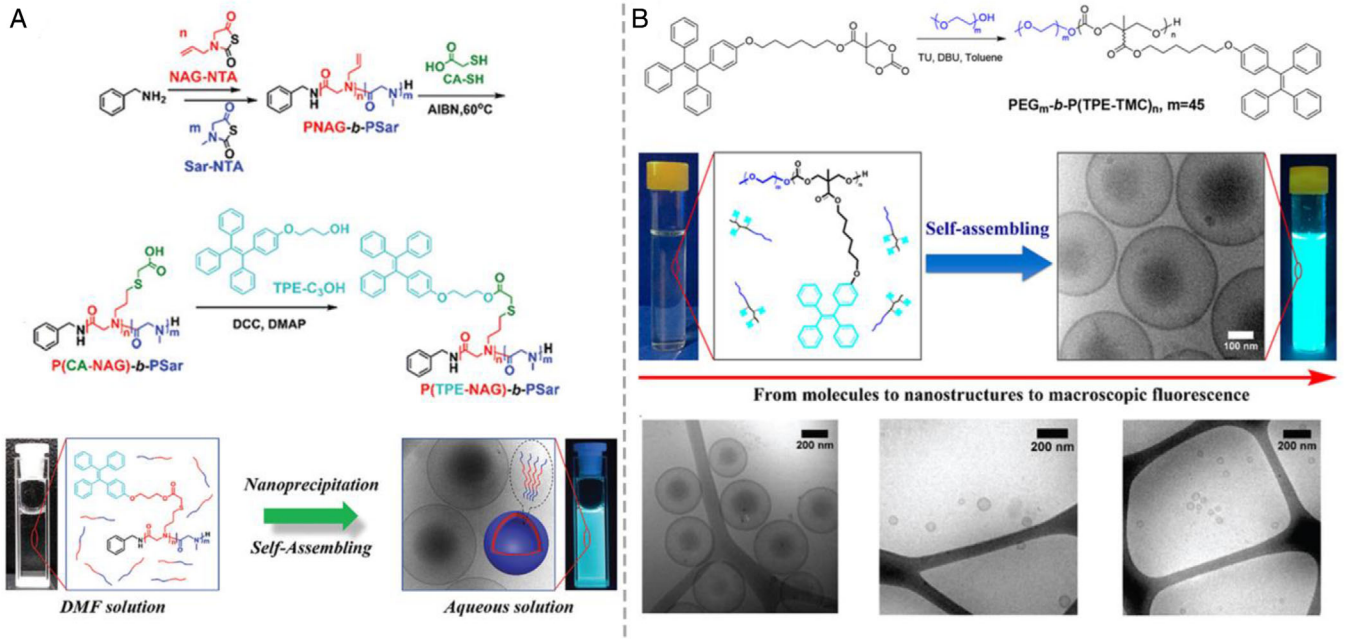

FIGURE 3 (A) Synthetic scheme of AIEgenic peptides, which are prepared via the ring-opening polymerization of N-thiocarboxyanhydride monomers, followed by thiol-ene chemistry modification, and subsequently post-polymerization with TPE groups via esterification. The resultant AIEgenic peptides are not emissive when dissolved in DMF, but upon self-assembly in aqueous medium, a boosted emission is observed. Reproduced from Ref. [106] with permission, Copyright 2019, the Royal Society of Chemistry. (B) Synthetic scheme of AIEgenic polycarbonates, which are prepared via ring-opening polymerization of tetraphenylethene (TPE)-based trimethylene carbonate (TMC) monomers; after assembly into polymersomes fluorescence is observed. Polymersome size can be controlled by changing the copolymer composition. Reproduced from Ref. [115] with permission, Copyright 2018, American Chemical Society

ranging from 17 to 24 kDa, and narrow Đ of ca. 1.1. The resultant polymers were readily self-assembled in pure aqueous solution due to their amphiphilic properties, which yielded spherical nanoparticles with a size range from 100–200 nm with strong fluorescence (Figure 2G,H); these nanoparticles were effectively utilized in cell imaging. Copolymerization strategies with other functional AIE monomers have also been reported by a number of research groups.[96–98]

In order to apply AIEgenic polymeric aggregates in a biomedical setting, a number of requirements involving minimal toxicity and efficient clearance in vivo should be met.[34,99–100] In this regard, amphiphilic polymers with inherent biodegradability are of interest.[8,101–104] Synthetic polypeptides are recognized as suitable candidates to prepare well-defined polymeric aggregates, providing several advantages including excellent biocompatibility, degradability and low cytotoxicity.[105] In 2019, Li et al. developed an approach to synthesize biodegradable AIEgenic polypeptides, based on the ring-opening polymerization (ROP) of N-substituted glycine N-thiocarboxyanhydride monomers (Figure 3A). Such ROP reaction was followed by chemical modification of the polymer through a thiol–ene radical addition reaction with mercaptoacetic acid to prepare carboxyl functionalized polypeptides.[106] Thereafter, AIE luminogens (e.g., TPEs) were attached to the polymer backbone via esterification-based post-polymerization. Self-assembly of the AIEgenic polymer was realized via a nanoprecipitation method with DMF/water as the co-solvent and a slow water addition process to induce polymer self-assembly in a more controlled way. The hydrophilic weight ratios of the block-co-polymers were able to be finely tuned (ranging from 18 to 38%), enabling the formation of particles with varied morphologies such as micelles and polymersomes. The resultant polypeptide-based polymeric aggregates had inherent low cytotoxicity and displayed strong AIE fluorescence in aqueous solution.

A versatile class of biodegradable copolymers for the engineering of amphiphilic polymeric aggregates with AIE features is based on poly(ethylene glycol)-poly(trimethylene carbonate) (PEG-PTMC).[107–108] The flexible PTMC and its copolymer derivatives are biocompatible and degradable and have appealing applications in the field of nanomedicine.[109] Unlike conventional polyesters, which produce acidic by-products after degradation, PTMC is recognized to have a unique degradation behavior, with resistance to non-enzymatic hydrolysis and non-acidic degradation by-products.[110–111] PTMC copolymers can be readily synthesized with a high level of control over polymer molecular weight, dispersity and end-group functionality via ROP of TMC-based monomers, using either organometallic catalysts or organic (acid/base) catalysts.[112] In addition, these copolymers are compelling for the construction of a range of polymer assemblies with controlled architectures.[113,114] For instance, in 2018, Li et al. developed a strategy to synthesize a series of amphiphilic AIEgenic block copolymers with well-defined compositions, via polymerizing a TPE coupled TMC monomer, using PEG_{45}-OH as the macro-initiator and 1,8-diazabicyclo[5.4.0]undec-7-ene (DBU) as catalyst (Figure 3B).[115] The integrated TPE moieties endowed the resulting polymers with obvious AIE characteristics: They were non-emissive in the dissolved state (e.g., in THF or dioxane solution), but the fluorescence was drastically increased upon aggregation or self-assembly. The formation of AIEgenic polymersomes was achieved via a solvent-switch method, in which water was slowly added into a polymer THF/dioxane solution, followed by an extensive dialysis process. The enhanced emission was associated

with the formation of vesicular aggregates that inhibit the intramolecular rotation of the TPE moieties. Importantly, the controlled ROP enabled fine-tuning of the hydrophilic and hydrophobic fractions, allowing control over their aggregation behavior and the size of the particles formed. With a decreased hydrophobic fraction, the average size of the spherical polymer vesicles, or polymersomes became smaller (from 450, 250 and 90 nm to 70 nm). Such ability to manipulate the physicochemical properties (e.g., size in this case) of the fluorescent polymersomes provides a structural base to optimize their behavior in a biological setting (such as in vivo circulation and cellular uptake).

In 2021, our group incorporated AIEgenic features in PTMC copolymers with a high density (>60 wt%) of a second-generation AIE functionality.[116] Unlike the early reported AIE compounds which only displayed solely emissive functionality, the second-generation here referred to are AIE molecules that can also be employed actively in therapies that rely on photochemical processes, such as PDT and PTT. This was achieved by polymerization of pentafluorophenyl derivatives of TMC to generate well-defined polymers that were modified (post-polymerization) with an amine-containing AIEgenic compound comprising both TPE and dicyanovinyl moieties. After self-assembly via a solvent-switch method, the prepared spherical polymersomes were effectively utilized in photosensitization and PDT. To equip AIEgenic aggregates with active targeting and enhance their biomedical utility, the same authors developed amphiphilic block copolymers composed of poly (ethylene glycol)-block-poly(caprolactone-gradient-TMC) (PEG-PCLgTMC), with a terminal block of tetraphenylethylene (TPE) pyridinium modified PTMC as a functional unit (PAIE).[117] This was achieved via a nucleophilic substitution-based post-polymerization. Whereas the TPE moiety provided PDT capacity to the polymer particles, the pyridinium group enabled the targeting of the mitochondria to enhance therapeutic performance.

2.2 | Host–guest engineering of AIEgenic supra-amphiphiles

Progress in the fabrication of AIEgenic amphiphilic polymers is primarily based on the covalent connection of AIE motifs and polymeric systems. Non-covalent supramolecular strategies utilizing host-guest interactions, employing macrocyclic molecules (such as crown ethers, cyclodextrins, calixarenes, cucurbits [CBs] and pillararenes), have emerged as alternative approaches to engineer AIEgenic aggregates.[118–125] Supramolecular complexation is an appealing engineering strategy for the construction of self-assembled, nanostructured materials, by allowing facile integration of functional elements without the need of multiple synthesis steps and complex purification processes.[126–128] In general, non-covalent bonds are inherently dynamic, and as such, the resultant supramolecular architectures can be readily equipped with stimuli-responsive features.[129–130] For instance, Sessler et al. developed a bola-type supra-amphiphile via supramolecular complexation between a water-soluble calix[4]pyrrole and a ditopic pyridine N-oxide derivative in aqueous media.[131] The host-guest interaction resulted in supramolecular self-assemblies with various morphologies, including multi-lamellar vesicles and micelles; both of which were responsive to pH and chemical competitors. Due to the aggregation, the resultant supra-amphiphile exhibited strong fluorescence in aqueous solutions, which allowed it to be applied for molecular recognition and controlled release studies.

Huang et al. constructed a pillararene-based AIEgenic amphiphilic supramolecular brush copolymer, utilizing the host-guest recognition between pillar[5]arene, pillar[5]arene with biotin modification and a 4,4′-bi-pyridinium tagged and TPE conjugated co-polymer, driven by charge transfer and hydrophobic interactions (Figure 4A).[122] The amphiphilic supramolecular brush copolymer was wrapped into core-shell structured nanoparticles, which were utilized as a self-imaging drug delivery vehicle by taking advantage of the self-assembly induced emission effect. The aromatic interaction between the AIEgenic group and anticancer drugs such as doxorubicin (DOX) also enabled a desirable level of encapsulation. Chen et al. developed an amphiphilic AIEgenic supramolecular brush copolymer based on CB[8]uril (CB[8]), poly-TPE modified with viologen moieties and PEGylated naphthol, employing the CB[8]-based ternary host−guest molecular recognition in an aqueous medium (Figure 4B).[132] Due to the instability of viologen in the presence of reducing agents or in low pH environments, the supramolecular host-guest interaction resulted in AIEgenic polymeric nanoparticles that were sensitive to the intracellular environment, allowing controlled release at the site of the target. Huang et al. fabricated functional fluorescent polymeric aggregates and investigated the influence of the aggregation morphology via host-guest-based supramolecular self-assembly (Figure 4C).[133] The fluorescent system was realized via a supramolecular graft strategy, based on a hydrophobic block consisting of polystyrene with pendent TPE moieties and paraquat units as a supramolecular guest group and a hydrophilic polymer composed of water-soluble poly(ethylene oxide) (PEO) terminated with a bis-(m-phenylene)-32-crown-10 unit containing two carboxy groups as host moiety. By adjusting the hydrophilic proportion, the supramolecular self-assembly yielded different aggregation morphologies, such as vesicles, wormlike micelles and spherical micelles (Figure 4C). In addition, the crown-paraquat recognition also induced pH-responsiveness, which could be utilized to realize controlled release of encapsulated drugs at specific tissues sites. The above results demonstrate that supramolecular engineering of AIEgenic nanoplatforms via host-guest interactions holds the capacity for developing advanced drug delivery systems.

2.3 | Morphology engineering of AIEgenic polymeric assemblies

Several well-defined morphologies such as spherical micelles, cylindrical micelles, lamellae, bilayer vesicles and inverse mesophases are formed as a result of the self-assembly of amphiphilic block copolymers in aqueous solutions.[134–138] The formation of such architectures is mainly driven by hydration of the hydrophilic blocks and interactions between the hydrophobic blocks to decrease the interfacial area and free energy.[45,139] Typically, both the

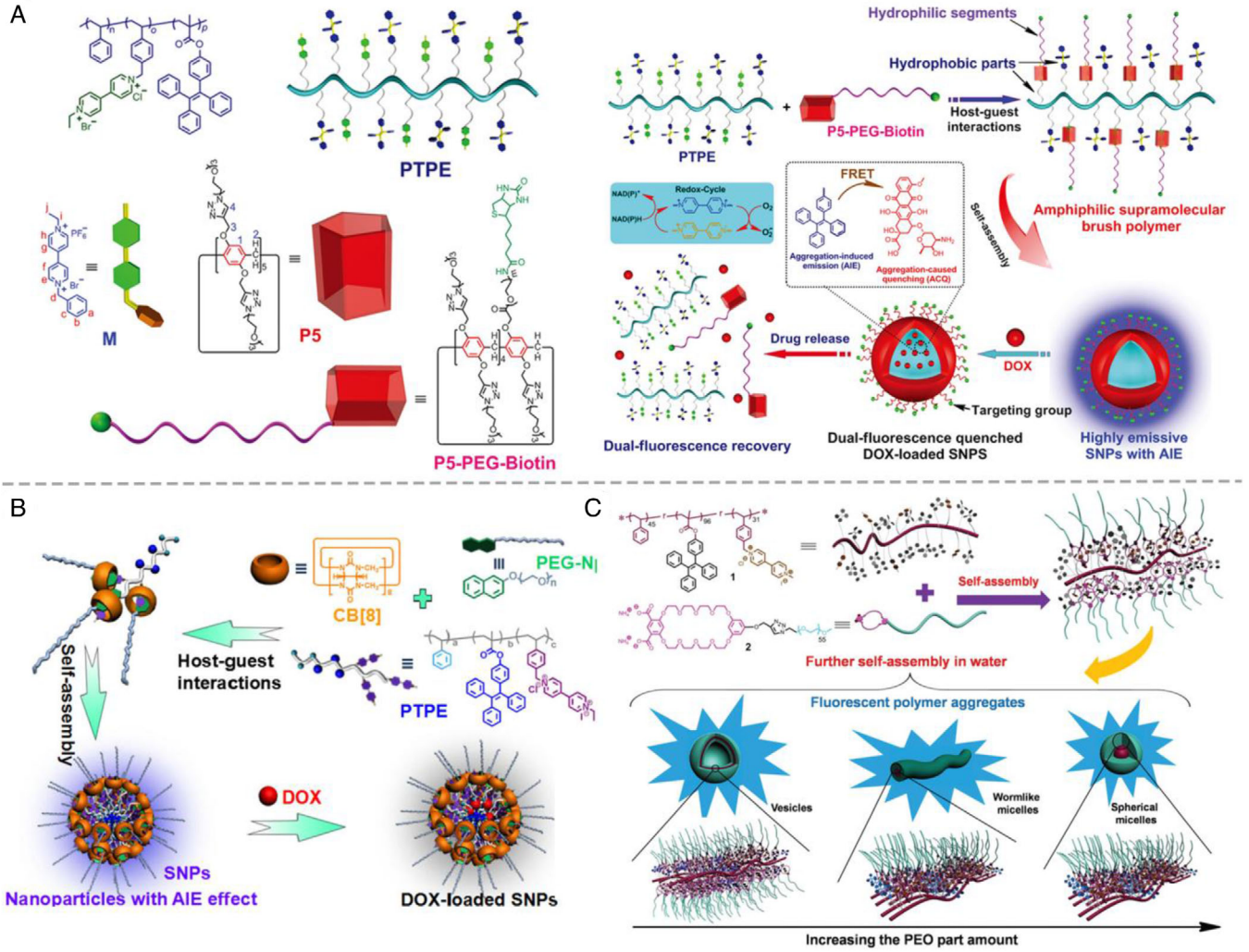

FIGURE 4 Formation of supramolecular AIEgenic self-assemblies via host-guest chemistry. (A) Left: Chemical structures of the supramolecular assembly consisting of the AIEgenic co-polymer carrying the 4,4′-bi-pyridinium guest moiety (M), and the two host compounds pillar[5]arene (P5) and pillar[5]arene with biotin (P5-PEG-biotin); Right: Schematic illustration of the formation of AIEgenic micelles self-assembled from the amphiphilic supramolecular brush copolymer. Reproduced from Ref. [122] with permission, Copyright 2016, the Royal Society of Chemistry. (B) Supramolecular AIEgenic nanocomplex constructed from a cucurbit[8]uril-based amphiphilic brush copolymer, which allows facile loading with aromatic drugs. Reproduced from Ref. [132] with permission, Copyright 2017 American Chemical Society. (C) Schematic representation of the supramolecular amphiphilic graft copolymer formed from host-guest interactions between the AIEgenic co-polymer and poly(ethylene oxide) (PEO) terminated with a bis-(m-phenylene)-32-crown-10, which self-assembles into different fluorescent polymeric aggregates in water. Reproduced from Ref. [133] with permission, Copyright 2015, the Royal Society of Chemistry

size and morphology of the nanoparticles can be fine-tuned by modifying the constituent building blocks and fabrication methods.[140–141] Morphology engineering of polymeric self-assemblies has emerged to yield a class of materials that can be used in medical devices and drug delivery systems.[142–144] In this context, AIEgenic aggregates based on amphiphilic polymers are very attractive.[41,145] Morphology engineering of AIEgenic assemblies for biomedical applications represents a challenge, due to their complex molecular structure. The ability of such AIEgenic aggregates to adopt a range of different morphologies, which could provide highly suitable candidates for nanomedicine applications, has been explored in recent years.[146–148] Yuan et al. developed a strategy to control the size and morphology of AIEgenic assemblies by changing the ratio of the incorporated components, including poly(N,N-dimethylaminoethyl methacrylate (PDMA), poly(benzyl methacrylate) (PBzMA) and poly(TPE) (PTPE) during RAFT dispersion copolymerization (Figure 5A).[149] A series of AIE-active polymeric assemblies including micelles, worms and vesicles were prepared via a polymerization-induced self-assembly approach in the presence of macro-chain-transfer agents. Initially, AIE-active micelles were formed with a lower percentage of BzMA–TPE blocks, in which the size of the particles was varied between 36 nm and 150 nm, by changing the length of the PDMA chain. With an increased hydrophobic BzMA–TPE block ratio, wormlike micelles, and vesicles were formed, which could be ascribed to the reduced hydrodynamic volume of the hydrophilic domain and the increased hydrophobic interactions (Figure 5B). In addition, the nanostructures displayed a morphological structure-correlated optical property, in which the fluorescence emission intensity at 480 nm of the AIE-vesicles was demonstrated to be higher than that of the other morphologies, including nanoworms and micelles (Figure 5C). The increased AIE emission could be related to the tightened chain packing and enhanced confinement of the embedded AIEgens in the hydrophobic core.

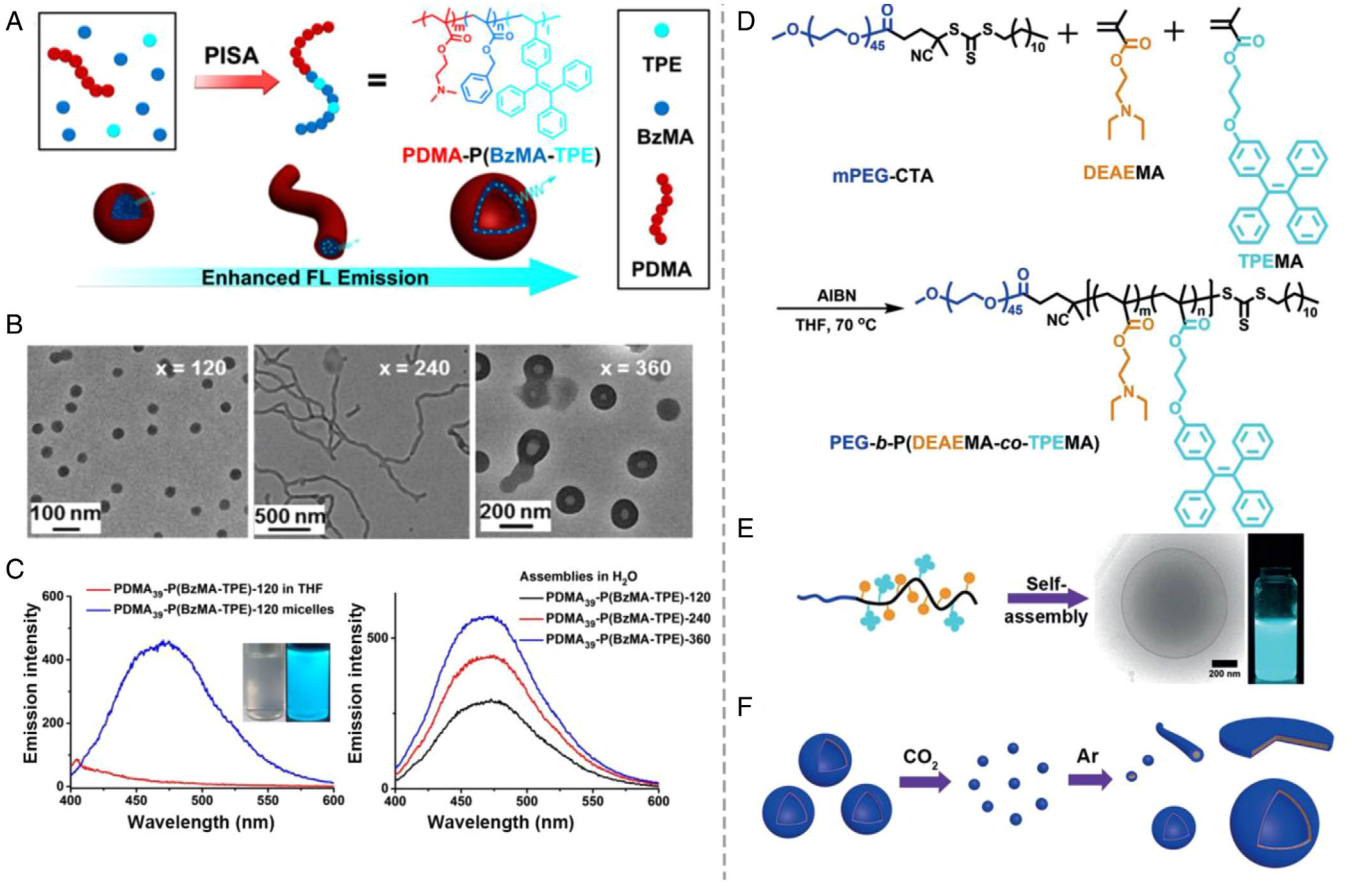

FIGURE 5 (A) Aggregation-induced emission (AIE)-based assemblies via polymerization-induced self-assembly (PISA), which results in a variety of morphologies depending on the feed of the monomers; (B) characterization of the different morphologies via transmission electron microscopy (TEM). (C) The photophysical behavior of AIE-based assemblies with different degrees of polymerization of BzMA and TPE. Reproduced from Ref. [149] with permission, Copyright 2017 American Chemical Society. (D) Synthetic procedure for the preparation of the CO_2-responsive amphiphilic block copolymer PEG-*b*-P((diethylamino)ethyl methacrylate [DEAEMA]-co-TPE functionalized methacrylate [TPEMA]). (E) The self-assembly of the AIEgenic amphiphilic block copolymer results in a vesicular morphology, as characterized with cryo-transmission electron microscopy (TEM), which displays intensive emission upon Ultraviolet (UV)-irradiation; (F) Upon CO_2 treatment, the polymeric self-assemblies undergo a transition to the micellar state, which can be reversed by treatment with Ar. Reproduced from Ref. [150] with permission, Copyright 2019, Wiley-VCH

Li et al. developed CO_2-responsive AIEgenic polymersomes constructed through nanoprecipitation of amphiphilic block copolymers in THF/water and dioxane/water systems.[150] The block copolymers were composed of PEG as the hydrophilic block and a copolymer of TPE functionalized methacrylate (TPEMA) and 2-(diethylamino)ethyl methacrylate (DEAEMA) as the hydrophobic block (Figure 5D). The polymersomes were prepared by a solvent-switch method, which resulted in bright fluorescent self-assemblies with intrinsic self-assembly induced emission (λ_{em} = 480 nm) (Figure 5E). Moreover, such polymersomes displayed CO_2 responsiveness, in which CO_2 bubbling into the AIE-polymersome solution resulted in a morphology transition from large spherical vesicles into smaller spherical micelles. This was attributed to the increased protonation of the PDEAEMA block, which led to a higher hydrophilic volume fraction and thus changed the polymer chain packing and self-assembly pathway (Figure 5F). Argon bubbling diminished the protonation effect, and, in turn, the particle morphology was restored to vesicles. The stimulus-responsiveness and morphology transition potential of this type of AIEgenic assemblies was utilized for applications as nanoreactors and controlled release systems. A limitation of this design was the non-biodegradable nature of the building blocks, as well as the short-wavelength emission and responsiveness to non-biological-related cues, which could hinder its in vivo applications.

3 | BIOLOGICAL APPLICATIONS OF AMPHIPHILIC AIEGEN-POLYMER AGGREGATES

Compared to small molecular AIE agents, amphiphilic AIEgen-polymer aggregates integrate the advantages of polymeric materials (that is, structural/functional diversity) with the specific features of AIE luminogens (that is, photostability), which make these nanomaterials of interest for biomedical applications.[30,32,151] In this section, we summarize and discuss the recent developments in applying amphiphilic AIEgen-polymer aggregates for (i) biosensing / bio-imaging / bio-tracking, (ii) drug delivery and theranostics and (iii) biomedical nanomotors.

3.1 | Biosensing, bio-imaging and bio-tracking

AIEgens are able to overcome the ACQ effect of traditional fluorophores and as such, AIEgenic nanocomplexes are widely used as probes and sensors for biosensing,

bio-imaging and bio-tracking.[152] Generally, AIEgens are hydrophobic, with poor solubility in aqueous and biological media. This issue was overcome by encapsulating them within lipid structures to enhance their water solubility.[153] Integration of AIEgens in amphiphilic polymer assemblies was recognized as an alternative effective strategy.[38–39,52,154–156] AIEgenic polymers, upon self-assembly, have been found to exhibit higher stability and durability than physically encapsulated AIEgens.[41,145] In addition, the resulting nanoparticles can be created in a range of different morphologies, with modifiable surfaces and enhanced biosafety.[157]

Due to their distinct emissive behavior in the solution and aggregated state, incorporation of AIE molecules/polymers is recognized as an excellent strategy for the design of 'turn on' fluorescent probes. For instance, Liu et al. developed AIEgenic polymers for DNA detection.[158] This was achieved by conjugating TPE moieties to a single-stranded oligonucleotide. The resulting TPE-nucleotide complex was tolerant to high ionic strength, enabling its application under hybridization conditions. Upon specific complementary binding of DNA in solution, fluorescence was enhanced, validating their potential to be used as fluorescent light-up probes for detecting single nucleotides in an effective way. Wang et al. designed and synthesized a series of AIE-active polymer probes for biothiol detection.[159] The AIE polymers were composed of disulfide-functionalized hyperbranched poly(amido amine) as the hydrophilic group, TPE as the hydrophobic core and a disulfide bond as the cleavable functional linkage. Upon exposure of the AIE polymer solution to glutathione or cysteine, 'turn-on' bright fluorescence was observed, which was attributed to the degradation of the dendritic structure and subsequent aggregation of the TPE moieties. This was further confirmed in in vitro experiments, highlighting the applicability of AIE polymers in biothiol detection in living cells.

AIEgenic polymer complex is also wildly utilized in the cell imaging. For instance, Wei et al. synthesized amphiphilic AIEgenic polymers through a combination of RAFT polymerization and a post-polymerization Hantzsch reaction, which self-assembled into fluorescent spherical organic nanoparticles (FONs) of ca. 100–200 nm in diameter (Figure 6A).[160] Such FONs exhibited excellent biocompatibility, good water dispersibility and bright fluorescence (λ_{em} = 460 nm) and were successfully utilized for bioimaging applications. Upon incubation of HepG2 cells with 10∼120 μg mL^{-1} particles, the cell viability was more than 90%. Confocal laser scanning microscopy (CLSM) proved that the FONs easily entered the cells by endocytosis of the HepG2 cells and were mainly located in the cytoplasm. The same group also prepared branched AIE-active fluorescent micelles via dynamic linkage of both phenylboronic acid terminated AIEgens and mPEG with a hydroxy-functional degradable hyperbranched polymer (Boltorn H40), which displayed strong orange-red fluorescence (λ_{ex}: 447 nm and / λ_{em}: 577 nm).[161] Because of the exceptional bright luminescence, alongside other properties such as water dispersibility and biocompatibility, the prepared AIEgenic nanoparticles were used for cell imaging, which stained HeLa cells effectively, with clearly visible intensive orange-red fluorescence. In addition, because of the unique AIE features, increasing the concentration of particles in the staining process enhanced the emission intensity in HeLa cells without sacrificing the specificity.

Jayakannan et al. constructed enzyme-responsive AIEgenic polysaccharide-based spherical polymersomes with a diameter of ca. 200 nm (Figure 6B).[162] The hydrophilic tail was composed of TPE-tagged polysaccharide-dextran, and the hydrophobic backbone was plant-based 3-pentadecyl phenol. Excellent encapsulation efficiency for both the hydrophilic Rose Bengal and the hydrophobic Nile Red fluorophores was demonstrated in the assembled polymersomes. Most importantly, the AIEgenic polymersomes exhibited fast intracellular delivery in live MCF-7 cells (less than 3 h). Enzyme-triggered cargo release was achieved at the intracellular level due to the enzymatic cleavage of the aliphatic ester linkage, which bridged the hydrophilic and hydrophobic units.[163] These examples demonstrate that AIEgenic enzyme-responsive polymersomes could be useful as intracellular delivery vehicles.

Wang et al., designed supramolecular AIEgenic gas-responsive vesicles (CO_2 and N_2) that were used as cell probes for cancer diagnosis (Figure 6C).[164] The polymeric vesicles were composed of the triblock copolymer poly-(4-undecoxy tetraphenyl ethylene methacrylate)-*b*-poly-((N-amidino)-(2,3-dihydro-1*H*-1,4-methyl-1,2,3-triazole)-(ethenyl benzene))-*b*-PEO (PTPE-*b*-PAD-*b*-PEO), containing a hydrophilic unit (PEO block), an amidine-containing CO_2-responsive segment (PAD block) and an AIEgen (PTPE block). The prepared AIE vesicles exhibited 'breathable' behavior in response to CO_2 and N_2. The PAD block was able to bind CO_2 which led to the expansion of the AIE vesicles, resulting in enhanced fluorescence of the PTPE block. The effect was reverted in the presence of N_2, which induced a decrease in the vesicle size, accompanied by a decrease in fluorescence intensity. Considering the high CO_2 concentration in cancerous tissue, efficient cancer cell imaging was achieved via these vesicles for a series of cancerous cell lines. For instance, they observed that the fluorescence intensity of GES-1 cells and 16HBE cells after incubation with the AIEgenic probe is low and dim. On the contrary, the AIEgenic probe incubated CNE1 cancer cells, 5–8F cancer cells, and HeLa cancer cells displayed much higher fluorescence intensity, which indicated that the as-prepared AIEgenic polymer probe can be used for cancer diagnosis by cellular imaging.

3.2 | Drug delivery and theranostics

AIEgenic self-assembled structures can effectively be used to encapsulate hydrophilic and hydrophobic components.[165–166] Combined with their tunable characteristics, such as morphology and size, and the ability to decorate their surface controllably with targeting ligands makes them well suited as drug delivery systems.[84,103] In this section, current progress in the areas of cargo transportation and theranostics using AIEgenic aggregates is described. AIEgenic micelles have been widely utilized to deliver aromatic drugs in nanomedicine studies, due to the beneficial π-π and hydrophobic interactions between the drugs and the AIEgens which inhibit cargo leakage during transportation.[81,83,167–172] In addition, AIEgenic micelles have been endowed with stimuli-responsive units

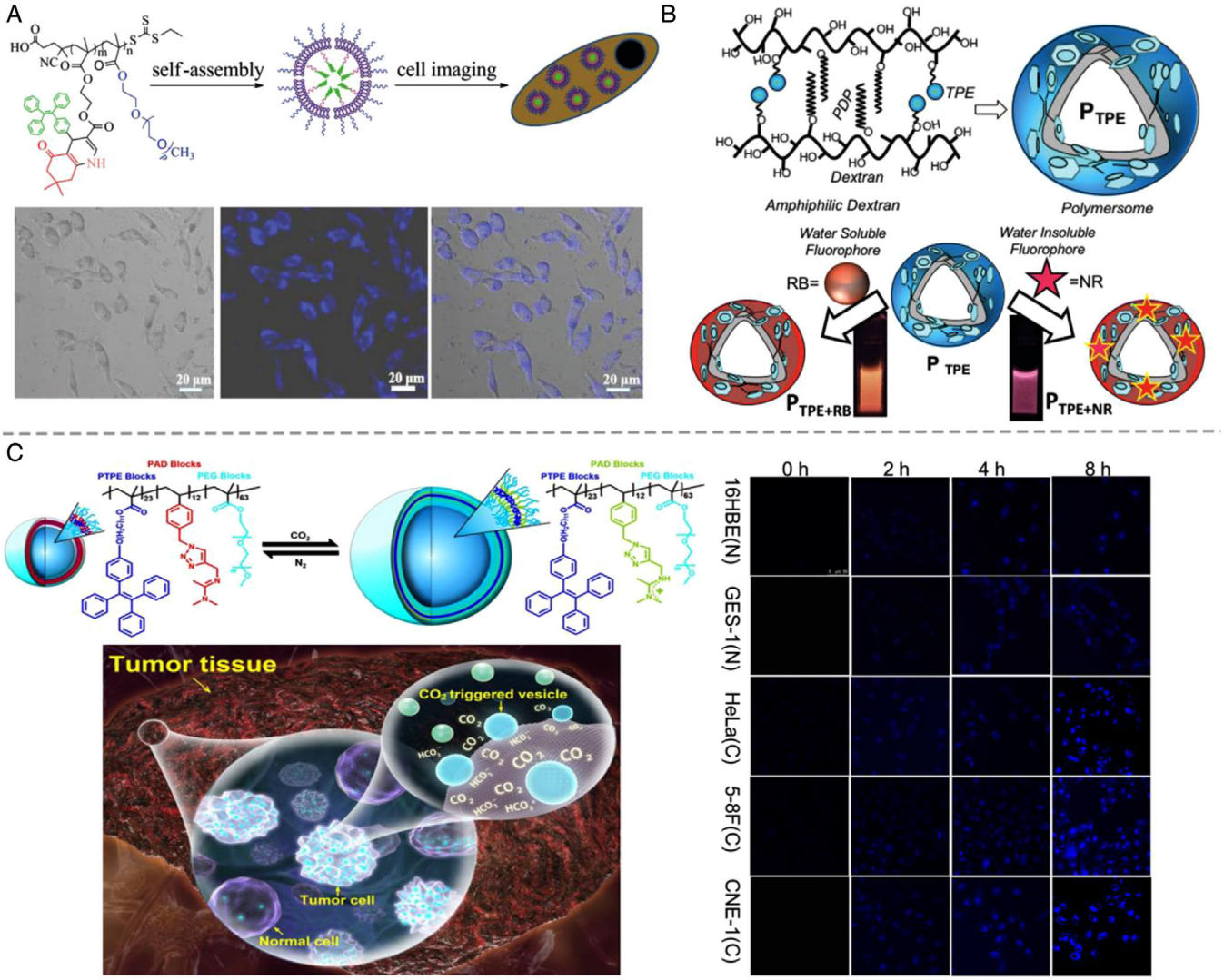

FIGURE 6 AIEgen-based polymer assemblies for bio-imaging and bio-tracking. (A) Schematic illustration of the preparation of AIEgen-conjugated amphiphilic polymers for HepG2 cell imaging. Reproduced from Ref. [160] with permission, Copyright 2017, the Royal Society of Chemistry. (B) Polymersomes from tetraphenylethylene (TPE) tagged polysaccharides display tailored emission upon loading with rhodamine and Nile Red. Reproduced from Ref. [162] with permission, Copyright 2021, Royal Society of Chemistry. (C) Schematic illustration of the responsiveness of supramolecular vesicles towards CO_2 and N_2, and the corresponding application to bio-imaging displaying different fluorescence intensity in different cell lines. Reproduced from Ref. [164] with permission, Copyright 2019 American Chemical Society

to achieve controlled release when the nanoparticles reached the targeted tissue microenvironment.[43,173] For instance, Zhao et al. reported AIEgenic micelles with enzyme responsive properties as drug carriers (Figure 7A). The authors synthesized the amphiphilic block copolymer, polyethylene glycol-*block*-poly(acrylic acid-*g*-TPE acrylate) (termed as PEG-*b*-P(AA-*g*-TPE)) in which the hydrophobic AIEgenic TPE was conjugated to the side chain of the hydrophilic polymer (CH_3O-PEG_{43}-*b*-PAA) via an ester linkage.[78] DOX was encapsulated during the self-assembly of the block copolymer into micelles, which was then released at the desired destination in the presence of esterase. The enzyme responsive feature guaranteed drug delivery to the site of the target, as unexpected drug burst release/leakage during transportation was avoided. The release process could be followed by determining the change of fluorescence resonance energy transfer (FRET) between the bright blue fluorescent AIE segment and DOX. CLSM studies with MCF-7 cells revealed efficient overlap of the red fluorescence of DOX and the aggregated TPE, demonstrating the delivery of DOX to cells through transportation via AIEgenic micelles. After treatment with AIEgenic micelles in the range of the tested concentrations for 48 h, the MCF-7 cells displayed a viability of approximately 98%, suggesting favorable biocompatibility. The DOX-loaded AIEgenic micelles effectively suppressed the growth of MCF-7 cells, decreasing their viability from 91% to 36% as the DOX concentration increased from 0.1 to 5.0 μg mL^{-1}.

AIEgenic polymeric micelles can also be prepared which respond to the acidic tumor microenvironment, while also allows a more effective deep tissue imaging using two-photon excitation.[174] For instance, Wang et al. prepared a novel type of AIEgenic copolymer consisting of mPEG as a hydrophilic block with a disulfide linkage, poly (2-azepane ethyl methacrylate) (PAEMA) as a pH-responsive hydrophobic block, and an AIEgenic block with two-photon excitable fluorescence (name as TBIS) (Figure 7B). The self-assembly of the AIEgenic amphiphilic copolymer was realized via a typical nano precipitation method (with THF/DMF, v/v 1:1, as organic phase), which yields core-shell micelles with an

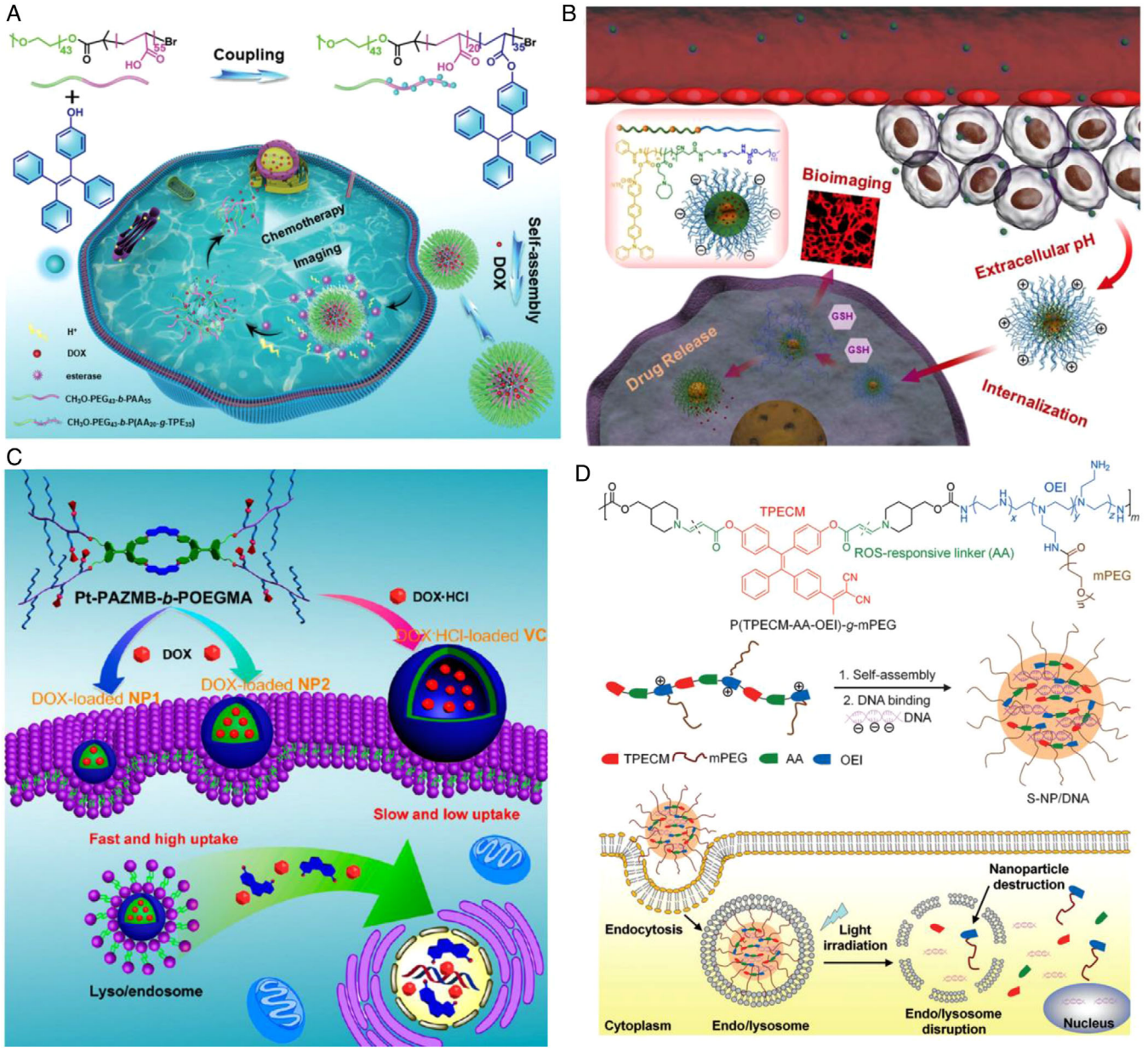

FIGURE 7 Delivery systems prepared from AIEgenic polymeric nanoparticles. (A) Enzyme-responsive polymeric micelles by self-assembly of AIEgen-coupled amphiphilic block copolymers for controlled drug release. Reproduced from Ref. [78] with permission: Copyright 2020, Royal Society of Chemistry. (B) pH-responsive and DOX-loaded AIE micelles for two-photon cell imaging and enhanced delivery to tumor cells. Reproduced from Ref. [174] with permission, Copyright 2019, Ivyspring International Publisher. (C) Schematic representation of AIEgenic nanoparticles loaded with DOX for in vitro and in vivo delivery. Reproduced from Ref. [175] with permission, Copyright 2017, American Chemical Society. (D) Schematic depiction of photoactivatable AIE polymer assemblies for light-controlled gene delivery. Reproduced from Ref. [171] with permission, Copyright 2015, John Wiley and Sons

average size of ~65 nm. Upon injection via the tail vein, the AIEgenic micelles were effectively accumulated in the tumor region in 4T1 tumor model-bearing mice. Exposure to the acidic tumor microenvironment resulted in charge-conversion of the AIEgenic micelles, which contributed to an enhanced cellular internalization. The integrated disulfide bond triggered the disassembly of the micelles in the presence of a high concentration of glutathione; this allowed the triggered release of encapsulated DOX inside the tumor cells. The excellent two-photon AIE active bioimaging of deep tumorous tissues using these responsive AIEgenic micelles was also confirmed. Further excellent antitumor efficacy with reduced side effects and the great two-photon bioimaging of cells and tissues make these AIEgenic micelles highly attractive as a candidate for cancer theranostics.

In order to further investigate the application of AIEgenic particles in vivo, Yu et al. prepared a synergistic responsive cargo carrier through the self-assembly of a four-armed amphiphilic copolymer into spherical nanoparticles (Figure 7C).[175] The authors prepared a glutathione (GSH)-responsive block copolymer (poly(azido-methyl benzoate)-*b*-poly(oligo ethylene glycol methacrylate), termed as Pt-PAZMB-*b*-POEGMA), wherein the emissive TPE-based bispyridyl ligands were the donors and acted as the fluorescent probe for live-cell imaging, while the acceptor 3,6-bis[trans-Pt(PEt_3)$_2$]phenanthrene (PhenPt) units were employed as an anticancer drug. Self-assembly of the amphiphilic copolymer was realized via a re-precipitation, dialysis and double-emulsion technique, which yielded nanoparticles of different sizes and morphologies (micelles

and vesicles). In addition, as a model anti-cancer drug, neutral DOX and DOX hydrochloride (DOX·HCl) were encapsulated in the assembled particles, which were used for cellular delivery through the endocytosis pathway. Controlled drug release was achieved by altering the amphiphilicity of the polymer via a GSH-triggered cascade elimination of the hydrophobic protection groups, which triggered particle disassembly (Figure 7C). An enhanced anti-tumor activity of drug-loaded AIEgenic particles was demonstrated upon intravenous administration of different formulations in HeLa tumor-bearing mice. After excision and weighing the tumors, tumor inhibition rates of DOX-loaded AIEgenic particles were found to be 82%, compared with 6% in the case of cisplatin and 20% in the case of pure DOX, further suggesting a better antitumor activity of DOX-loaded AIEgenic particles.

Another interesting application of AIEgenic nanoparticles is gene delivery, which was explored by Liu and coworkers. The authors developed a photoactive AIEgenic polymer comprising an AIEgenic photosensitizer and oligoethylenimine (OEI) conjugated with a reactive oxygen species (ROS) responsive linker (Figure 7D).[171] Interestingly, these AIEgenic nanovectors induced endo/lysosomal escape and DNA unpacking upon light irradiation, which in turn led to the efficient delivery of DNA to the cytosol. Moreover, compared to commercial poly(ethylene imine) (MW 24 kDa), AIEgenic nanovectors with a ROS-responsive linker displayed a ca. 50% higher transfection efficiency. The AIEgenic nanovector developed in this report offers a robust strategy for gene delivery; such strategy could be applied in other delivery applications such as siRNA, as well as drug delivery to the cytosol.

Besides the compelling application of amphiphilic polymeric AIEgenic aggregates in the field of drug delivery, they also are of high added value in the area of theranostics.[35,176–178] For instance, our group designed a well-defined biodegradable AIE polymersome with inherent fluorescence and targeting capacity for enhanced PDT (Figure 8A).[117] The AIEgenic biodegradable amphiphilic polymer was composed of poly(ethylene glycol)-block-poly(caprolactone-gradient-TMC) (PEG-P(CLgTMC)) to which TPE pyridinium AIE units were conjugated. After self-assembly via a direct hydration method, spherical AIEgenic polymersomes were obtained with a diameter of ca. 120 nm. Such polymersomes displayed intrinsic fluorescence ($\lambda_{ex}/\lambda_{em}$: 405 nm / 650 nm), which facilitated their use in cell imaging and tracking. Importantly, these polymersomes showed specific mitochondria-targeting, which was attributed to the presence of the pyridinium moieties. These pyridinium units allowed precise transportation of encapsulated photosensitizers, BODIPY in this case, and thus improved the therapeutic efficiency with negligible side effects. In vitro tests demonstrated enhanced generation of cytotoxic ROS upon near infrared (NIR) irradiation, which is promising for anticancer therapy. The therapeutic capacity of these AIEgenic polymersomes was further evaluated in vivo with subcutaneous A549 tumor-bearing nude mice. Tumor growth was significantly inhibited after treatment with photosensitizer-loaded AIE-polymersomes and light irradiation, as evident by measuring the tumor volume and weight (Figure 8A). Typical TdT-mediated dUTP nick end-labelling staining of tumor sections excised from the tumor-bearing mice after 18 days of treatment provided further evidence of more efficient tumor growth inhibition by photosensitizer-loaded AIE-polymersomes with NIR light irradiation.

Liu et al. exploited AIE-based polymers for self-selective targeting and antimicrobial resistance (Figure 8B).[179] Through copper-catalyzed atom transfer radical polymerization (ATRP), acrylic polymers with AIE features were synthesized. Three important components were included in this polymer, namely, (2-(methacryloyloxy)ethyl) trimethyl ammonium chloride (TMAEMC), the AIE moiety (TPAPy) and (2-(methacryloyloxy)ethyl)dimethyl-(3-sulfopropyl)ammonium hydroxide (DMAPS). As a cation, TMAEMC was able to bind to the negatively charged bacterial surface. DMAPS was utilized as a spacer between the binding cationic sections, as well as to enhance the aqueous solubility of the polymer. Most importantly, the AIE moiety was important for fluorescent imaging and PDT (Figure 8B). In this way, the AIEgenic polymers were capable of matching and recognizing a wide range of pathogenic bacteria, which allowed selective bacterial imaging via 'turn on' fluorescence, as well as killing bacteria via PDT upon laser irradiation. Similarly, Chen et al. reported a strategy to target bacteria that were intracellularly active in macrophages. For this purpose, they developed mannose-grafted polymers containing TPE AIEgen units and enzyme-responsive segments for the assembly of AIEgenic nanoparticles.[180] Such nanoparticles were able to encapsulate Fe^{3+}($D_{Fe}C$) conjugated deferoxamine-ciprofloxacin via π-π stacking / hydrophobic interactions (Figure 8C). Due to the overlapping absorption of $D_{Fe}C$, the fluorescence of the AIEgenic nanoparticles was initially quenched via the FRET. The mannose moieties allowed efficient uptake of the as-prepared AIE nanoparticles by infected macrophages. Macrophagic uptake was followed by the release of the encapsulated payloads ($D_{Fe}C$) in the presence of intracellular lipase and phosphatase secreted by intracellular bacteria. With the enzyme-triggered release of $D_{Fe}C$, the fluorescence emission of the nanoparticles was turned on as the FRET effect was significantly alleviated. In this way, cellular uptake and intracellular controlled release were tracked and monitored in situ by detecting changes in fluorescence. Most importantly, the controlled release allowed an effective deferoxamine-mediated antibacterial therapy.

3.3 | Nanomotors featuring AIE properties

A recent development in the field of nanomedicine is to create nanoparticles with the ability to undergo non-Brownian autonomous motion.[181–183] This feature can be useful to achieve deeper tissue penetration and to overcome tissue and cellular carriers more effectively. As such, they can be beneficial for diagnostics and drug delivery.[184] A variety of driving forces, either chemical (that is, catalytic reaction),[185–187] physical (that is, light/ultrasound/electricity/magnetic fields),[188–192] or even biological (that is, motile cells),[193–194] to power the propulsion of such motors have been investigated.[195–198] For biomedical applications, light-driven nanomotors have drawn much attention, as light permits motion control whilst allowing extra therapeutic effects such as PDT and PTT.[199–201] AIEgenic aggregates were also used as the

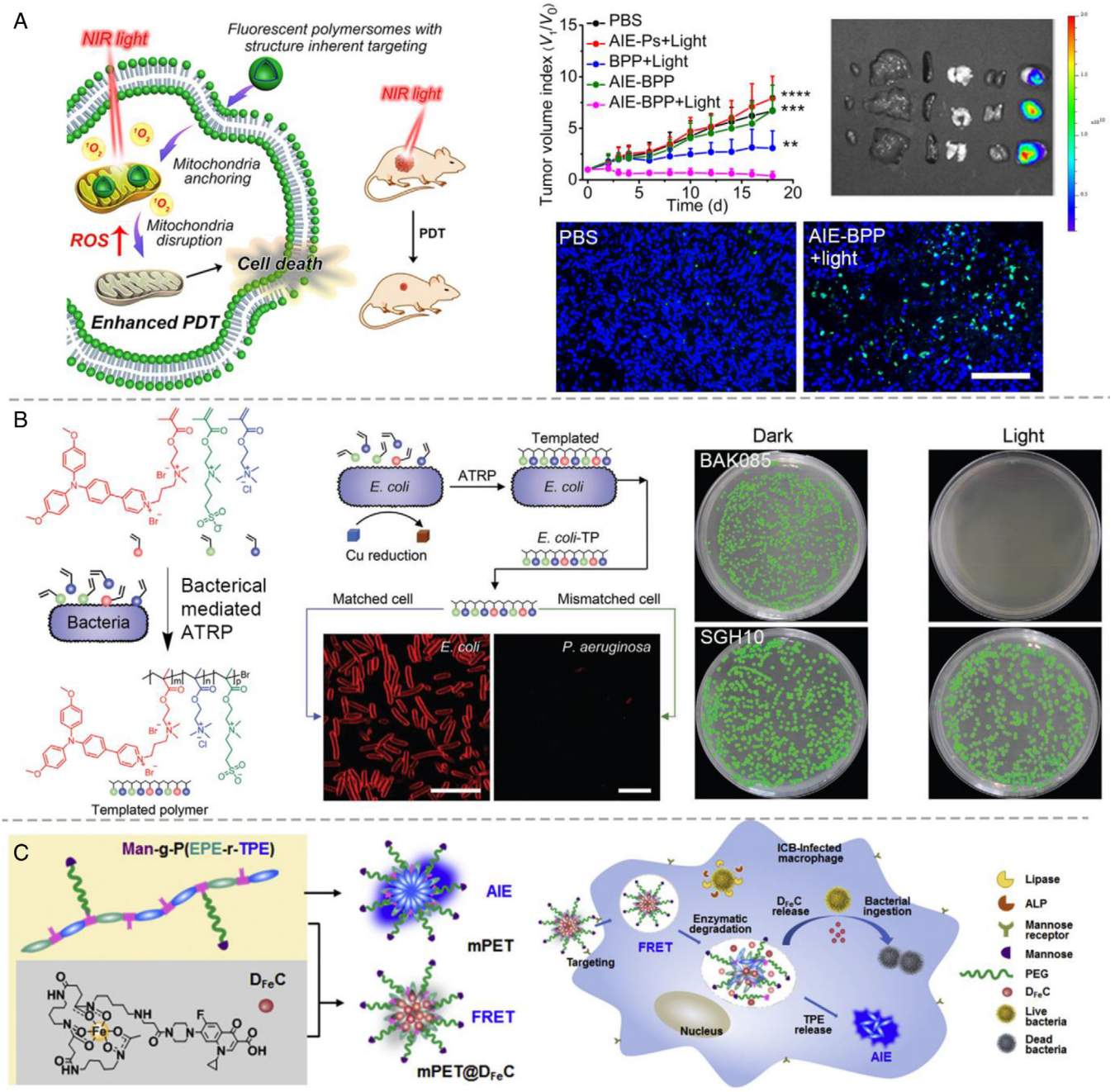

FIGURE 8 (A) AIE-polymersomes (AIE-BPP) loaded with photosensitizers which are capable of mitochondrial targeting and photodynamic therapy (PDT). The therapeutic effect is evaluated by monitoring the tumor volume index, tumor weight, and TdT-mediated dUTP nick end-labelling (TUNEL) staining of tumor sections after PDT treatment. Reproduced from Ref. [117] with permission, Copyright 2021, John Wiley and Sons. (B) Schematic illustration of bacteria-mediated atom transfer radical polymerization (ATRP) to create an AIE-functional copolymer. The aggregation-induced emission (AIE) features can be used for selective imaging and bacterial killing. Reproduced from Ref. [179] with permission, Copyright 2020, John Wiley and Sons. (C) Schematic depiction of the assembly of nanoparticles with AIE properties for enzyme-responsive release and deferoxamine ($D_{Fe}C$)-mediated intracellular bacterial destruction. Reproduced from Ref. [180] with permission, Copyright 2020, Elsevier

building blocks for nanomotor design. Our group developed a phototactic/phototherapeutic hybrid nanomotor by the self-assembly of biodegradable block copolymers comprising AIE motifs into polymersomes. The block copolymer (PEG-$PTMC_{AIE}$) was synthesized by conjugating the hydrophilic PEG with AIEgenic (comprising both tetraphenylethylene and dicyanovinyl moieties, TPEDC)-rich poly(TMC) (PTMC). After assembly with a solvent switch method, AIE-polymersomes were obtained after extensive dialysis to remove the organic solvent. These nanoparticles were subsequently covered with a hemispherical gold shell using sputter coating, forming AIE-polymersome nanomotors (Figure 9).[116] The asymmetric gold layer allowed harnessing two-photon near-infrared radiation as a trigger for motion, as a result of the temperature gradient that was generated around the nanomotors.[202–204] Due to the motors' asymmetry, motion behavior was highly directional. Interestingly, such hemispherical gold shells also served as energy sink for the AIEgenic fluorescence. The combination of an asymmetric gold shell and AIE moieties in one system resulted in enhanced motion as a result of increased thermophoresis. Moreover, synergistic phototaxis was achieved when

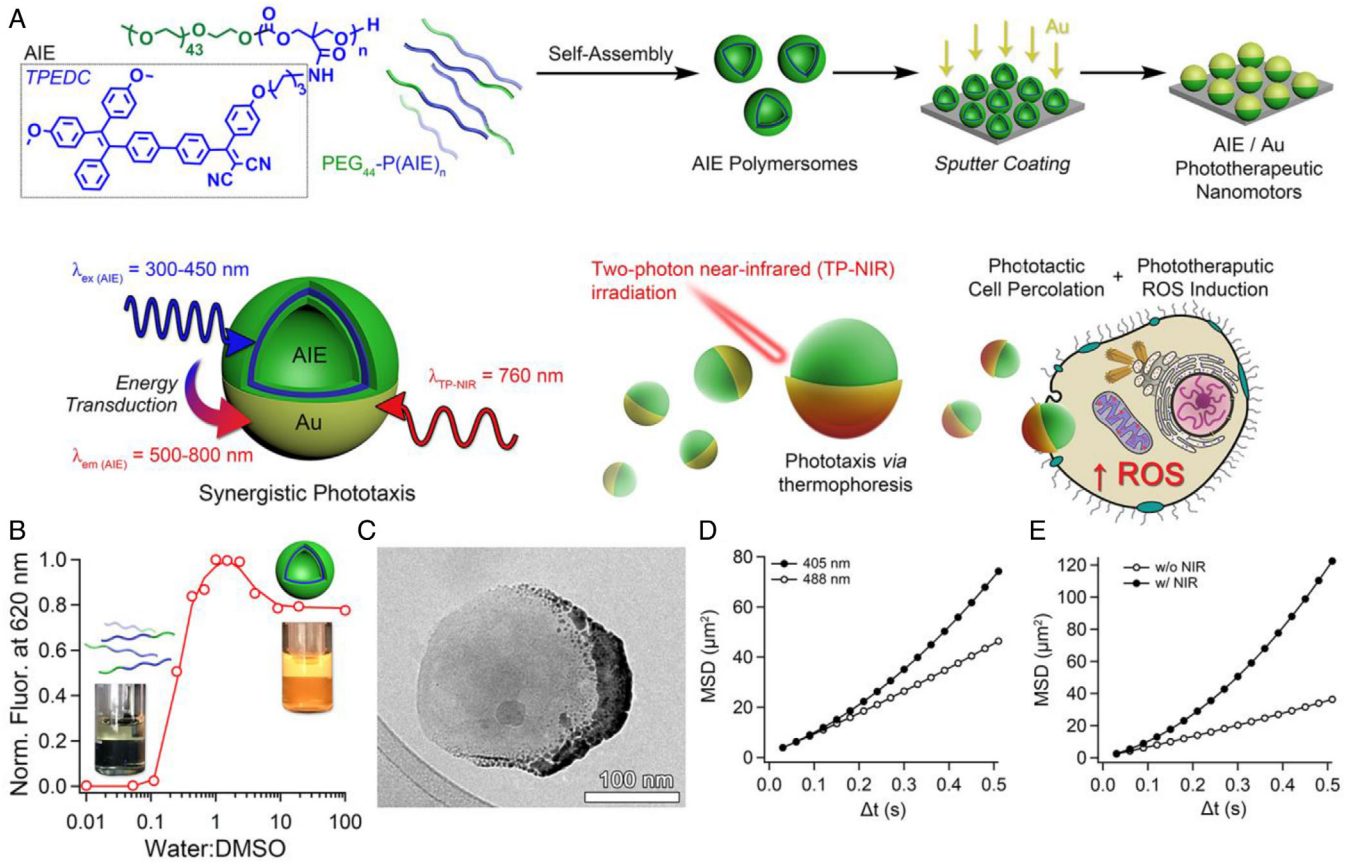

FIGURE 9 (A) Schematic illustration of aggregation-induced emission (AIE)-functional nanomotors with synergistic phototaxis. Polymersomes are prepared by the self-assembly of biodegradable amphiphilic copolymers composed of AIEgenic TPEDC and PEG_{44}-poly(trimethylene carbonate) (PTMC); the particles are coated with a hemispherical gold layer using a sputter coating approach. (B) Aggregation-induced fluorescence of AIE conjugate block copolymers due to self-assembly induced by water addition ($\lambda_{ex}/\lambda_{em}$ = 373 nm / 617 nm). (C) Cryogenic transmission electron microscopy (Cryo-TEM) image of an AIE-polymersome nanomotor. The dark patches represent the hemispherical gold shell. (D) Mean squared displacement (MSD) measured using nanosight tracking, comparing the motion of AIE-polymersome nanomotors under 405 nm and 488 nm irradiation. Upon 405 nm irradiation, energy transduction to the gold shell leads to directed motion. (E) Mean squared displacement (MSD) of AIE-polymersome nanomotors with/without NIR laser irradiation. Reproduced from Ref. [116] with permission, Copyright 2021, Springer Nature

the particles were exposed to two-photon laser irradiation (λ_{ex} = 760 nm) (Figure 9D,E). Due to the miniaturized size and their active motion, nanomotors facilitate effective interactions with cells and tissues.[184,198,205–208] The use of AIE-polymersome nanomotors for biomedical applications, especially in PDT, was exploited by the same research group. While AIEgens in the nanomotors allowed for the fluorescent imaging and generation of ROS, the gold hemispherical shells resulted in a photothermal anti-cancer effect. Interestingly, such light-driven motors were able to traverse cellular membranes (with HeLa cells), resulting in their efficient introduction into cancerous cells and consequent delivery of cargo. Following treatment with AIE nanomotors, after 200 s of two-photon NIR (TP-NIR) irradiation, significant disruption of the cell wall was observed. This was likely due to the effect of the highly propulsive nanomotors that caused localized percolation. In control experiments, after 200 s of TP-NIR irradiation, AIE polymersomes only induced a small degree of ROS in cells. In sharp contrast, HeLa cells treated with AIE nanomotors showed high levels of ROS after only 48 s irradiation. Critical loss of cellular activity after treatment with the AIE motors was also confirmed, indicated by the diminished calcein fluorescence and increased emission of propidium iodide.

4 | CONCLUSION AND PERSPECTIVE

AIEgenic molecules have emerged as a novel type of fluorescent materials, which, upon their aggregation, become fluorescent with enhanced emission compared to the dissolved state. A recent development is the integration of AIEgenic moieties with polymeric building blocks for the formation of intrinsically fluorescent polymer assemblies. This allows full exploration of the versatile polymer science toolbox, with control over chemical composition, chain length and functional groups, along with topological features. This review has summarized the recent progress on the design and synthesis of the AIEgenic amphiphilic polymers, using either polymerization or post-polymerization methods. Furthermore, the preparation of AIEgenic polymeric aggregates can also be obtained via facile non-covalent supramolecular host-guest interactions. Of particular interest is the ability of AIEgenic aggregates to acquire properties such as environmental responsiveness and adaptive morphology. When equipped with therapeutic modalities, these responsive AIEgenic assemblies have been successfully applied in diverse biomedical applications such as cell imaging, vascular imaging, long-term tracking, disease diagnosis and cancer therapy.

Despite the current progress in designing AIEgenic polymeric nanoparticles, there are a number of aspects that need attention to fulfil the requirements of practical use in a physiological environment and ensure successful application in nanomedicine. For instance, TPE, the basic AIE moiety with λ_{em} around 480 nm, is commonly utilized in the construction of AIEgenic nanostructures. However, from a biomedical application point of view, AIEgens with near-infrared or multiphoton absorption are more desirable due to their deeper tissue penetration capabilities and lower signal-to-noise ratio. RAFT or ATRP based polymerization approaches are popular methods to prepare AIEgenic building blocks that yield assemblies with controlled size and stimulus-responsiveness. However, their non-biodegradable nature can limit their use in in vivo applications. Although the concept of responsiveness to external cues at the target tissue site of action has already been demonstrated, this feature is still underexplored and offers therefore much potential to further improve biomedical performance. The same holds for AIEgenic aggregates with controlled morphology (e.g., polymersomes, micelles, nanoworms). An important step forward is therefore to develop robust approaches to create AIEgenic assemblies from biodegradable and biocompatible materials such as polypeptides, polyesters and polycarbonates, with control over topology and responsiveness.

Only recently AIEgens and polymer chemistry have been merged, and it is to be expected that the abovementioned aspects can be conveniently integrated in the next generation of AIEgenic polymeric nanoparticles. From a synthetic point of view, there do not seem to be any intrinsic limitations to the construction of these building blocks as AIEgens have shown to be highly compatible with the readily available polymer synthesis toolbox. We expect that the fabrication of smart luminescent materials that combine control over topology and other physicochemical features with unique emission properties, will lead to a versatile nanomedicine platform that is primed for further biomedical applications.

ACKNOWLEDGEMENTS

The authors would like to acknowledge the ERC Advanced Grant Artisym (grant number: 694120), the Dutch Ministry of Education, Culture and Science (gravitation program 024.001.035), the NWO-NSFC Advanced Materials (project 792.001.015) and the European Union's Horizon 2020 research and innovation program Marie Sklodowska-Curie Innovative Training Networks Nanomed, (grant number: 676137) for funding.

CONFLICT OF INTEREST

The authors declare no competing financial interests.

ORCID

Jan C. M. van Hest https://orcid.org/0000-0001-7973-2404

REFERENCES

1. P. P. Ghoroghchian, P. R. Frail, K. Susumu, D. Blessington, A. K. Brannan, F. S. Bates, B. Chance, D. A. Hammer, M. J. Therien, *Proc. Natl. Acad. Sci. U. S. A.* **2005**, *102*, 2922.
2. M. Chen, M. Yin, *Prog. Polym. Sci.* **2014**, *39*, 365.
3. M. Elsabahy, G. S. Heo, S.-M. Lim, G. Sun, K. L. Wooley, *Chem. Rev.* **2015**, *115*, 10967.
4. J. Tian, W. A. Zhang, *Prog. Polym. Sci.* **2019**, *95*, 65.
5. T. Kowada, H. Maeda, K. Kikuchi, *Chem. Soc. Rev.* **2015**, *44*, 4953.
6. S. J. Zhu, R. Tian, A. L. Antaris, X. Y. Chen, H. J. Dai, *Adv. Mater.* **2019**, *31*, 1900321.
7. Y. Li, T.-y. Lin, Y. Luo, Q. Liu, W. Xiao, W. Guo, D. Lac, H. Zhang, C. Feng, S. Wachsmann-Hogiu, J. H. Walton, S. R. Cherry, D. J. Rowland, D. Kukis, C. Pan, K. S. Lam, *Nat. Commun.* **2014**, *5*, 4712.
8. N. Kamaly, B. Yameen, J. Wu, O. C. Farokhzad, *Chem. Rev.* **2016**, *116*, 2602.
9. J. P. Celli, B. Q. Spring, I. Rizvi, C. L. Evans, K. S. Samkoe, S. Verma, B. W. Pogue, T. Hasan, *Chem. Rev.* **2010**, *110*, 2795.
10. T. Eder, T. Stangl, M. Gmelch, K. Remmerssen, D. Laux, S. Höger, J. M. Lupton, J. Vogelsang, *Nat. Commun.* **2017**, *8*, 1641.
11. Y. Huang, J. Xing, Q. Gong, L.-C. Chen, G. Liu, C. Yao, Z. Wang, H.-L. Zhang, Z. Chen, Q. Zhang, *Nat. Commun.* **2019**, *10*, 169.
12. J. R. Lakowicz, *Principles of Fluorescence Spectroscopy*, 3rd ed., Springer, New York **2006**.
13. D. Zhai, W. Xu, L. Zhang, Y.-T. Chang, *Chem. Soc. Rev.* **2014**, *43*, 2402.
14. S. S. Lucky, K. C. Soo, Y. Zhang, *Chem. Rev.* **2015**, *115*, 1990.
15. V.-N. Nguyen, Y. Yan, J. Zhao, J. Yoon, *Acc. Chem. Res.* **2021**, *54*, 207.
16. K. T. Nguyen, Y. Zhao, *Acc. Chem. Res.* **2015**, *48*, 3016.
17. J. Jin, Y. Zhu, Z. Zhang, W. Zhang, *Angew. Chem. Int. Ed.* **2018**, *57*, 16354.
18. Y. Hong, J. W. Y. Lam, B. Z. Tang, *Chem. Soc. Rev.* **2011**, *40*, 5361.
19. H. Wang, E. G. Zhao, J. W. Y. Lam, B. Z. Tang, *Mater. Today* **2015**, *18*, 365.
20. H. K. Zhang, Z. Zhao, A. T. Turley, L. Wang, P. R. McGonigal, Y. J. Tu, Y. Y. Li, Z. Y. Wang, R. T. K. Kwok, J. W. Y. Lam, B. Z. Tang, *Adv. Mater.* **2020**, *32*, 2001457.
21. H. Chen, M.-H. Li, *Chin. J. Polym. Sci.* **2019**, *37*, 352.
22. J. Mei, Y. N. Hong, J. W. Y. Lam, A. J. Qin, Y. H. Tang, B. Z. Tang, *Adv. Mater.* **2014**, *26*, 5429.
23. J. Mei, N. L. C. Leung, R. T. K. Kwok, J. W. Y. Lam, B. Z. Tang, *Chem. Rev.* **2015**, *115*, 11718.
24. Z. J. Zhao, B. R. He, B. Tang, *Chem. Sci.* **2015**, *6*, 5347.
25. H. T. Feng, J. W. Y. Lam, B. Z. Tang, *Coord. Chem. Rev.* **2020**, *406*, 213142.
26. Z. Zhao, H. K. Zhang, J. W. Y. Lam, B. Z. Tang, *Angew. Chem. Int. Ed.* **2020**, *59*, 9888.
27. J. Yu, X. Sun, F. Cai, Z. Zhu, A. Qin, J. Qian, B. Tang, S. He, *Opt. Lett.* **2015**, *40*, 2313.
28. D. Li, W. Qin, B. Xu, J. Qian, B. Z. Tang, *Adv. Mater.* **2017**, *29*, 1703643.
29. D. Ding, K. Li, B. Liu, B. Z. Tang, *Acc. Chem. Res.* **2013**, *46*, 2441.
30. R. T. K. Kwok, C. W. T. Leung, J. W. Y. Lam, B. Z. Tang, *Chem. Soc. Rev.* **2015**, *44*, 4228.
31. J. Liang, B. Tang, B. Liu, *Chem. Soc. Rev.* **2015**, *44*, 2798.
32. J. Qian, B. Z. Tang, *Chem* **2017**, *3*, 56.
33. G. Chen, I. Roy, C. Yang, P. N. Prasad, *Chem. Rev.* **2016**, *116*, 2826.
34. W. R. Sanhai, J. H. Sakamoto, R. Canady, M. Ferrari, *Nat. Nanotechnol.* **2008**, *3*, 242.
35. G. X. Feng, B. Liu, *Acc. Chem. Res.* **2018**, *51*, 1404.
36. M. Chen, A. J. Qin, J. W. Y. Lam, B. Z. Tang, *Coord. Chem. Rev.* **2020**, *422*, 213472.
37. N. Song, Z. J. Zhang, P. Y. Liu, Y. W. Yang, L. Wang, D. Wang, B. Z. Tang, *Adv. Mater.* **2020**, *32*, 2004208.
38. R. Hu, N. L. C. Leung, B. Z. Tang, *Chem. Soc. Rev.* **2014**, *43*, 4494.
39. X. Zhang, K. Wang, M. Liu, X. Zhang, L. Tao, Y. Chen, Y. Wei, *Nanoscale* **2015**, *7*, 11486.
40. S. Dalapati, C. Gu, D. L. Jiang, *Small* **2016**, *12*, 6513.
41. R. Hu, A. J. Qin, B. Z. Tang, *Prog. Polym. Sci.* **2020**, *100*, 101176
42. J. Li, J. Wang, H. Li, N. Song, D. Wang, B. Z. Tang, *Chem. Soc. Rev.* **2020**, *49*, 1144.
43. J. Zhang, B. Z. He, Y. B. Hu, P. Alam, H. K. Zhang, J. W. Y. Lam, B. Z. Tang, *Adv. Mater.* **2021**, *33*, 2008071
44. J. K. Kim, S. Y. Yang, Y. Lee, Y. Kim, *Prog. Polym. Sci.* **2010**, *35*, 1325.
45. Y. Mai, A. Eisenberg, *Chem. Soc. Rev.* **2012**, *41*, 5969.
46. A. Rösler, G. W. M. Vandermeulen, H.-A. Klok, *Adv. Drug Deliv. Rev.* **2012**, *64*, 270.
47. Y. Zhao, F. Sakai, L. Su, Y. Liu, K. Wei, G. Chen, M. Jiang, *Adv. Mater.* **2013**, *25*, 5215.
48. B. Li, T. Chen, Z. Wang, Z. Guo, J. Peña, L. Zeng, J. Xing, *J. Mater. Chem. B* **2020**, *8*, 2431.

49. D. Ding, R. T. K. Kwok, Y. Yuan, G. Feng, B. Z. Tang, B. Liu, *Mater. Horiz.* **2015**, *2*, 100.
50. T. Xue, X. Jia, J. Wang, J. Xiang, W. Wang, J. Du, Y. He, *Chem. Eur. J.* **2019**, *25*, 9634.
51. J. Yang, Q. Peng, R. Xue, Z. Li, X. Zheng, *Mater. Chem. Front.* **2021**, *5*, 1806.
52. B. Li, T. He, X. Shen, D. Tang, S. Yin, *Poly. Chem.* **2019**, *10*, 796.
53. X.-Y. Lou, Y.-W. Yang, *Aggregate* **2020**, *1*, 19.
54. A. Nicol, R. T. K. Kwok, C. Chen, W. Zhao, M. Chen, J. Qu, B. Z. Tang, *J. Am. Chem. Soc.* **2017**, *139*, 14792.
55. Y. Yuan, C.-J. Zhang, B. Liu, *Chem. Comm.* **2015**, *51*, 8626.
56. H. Cao, Z. Yue, H. Gao, C. Chen, K. Cui, K. Zhang, Y. Cheng, G. Shao, D. Kong, Z. Li, D. Ding, Y. Wang, *ACS Nano* **2019**, *13*, 3522.
57. F. Hu, D. Mao, Kenry, X. Cai, W. Wu, D. Kong, B. Liu, *Angew. Chem. Int. Ed.* **2018**, *57*, 10182.
58. T. Zhang, Y. Li, Z. Zheng, R. Ye, Y. Zhang, R. T. K. Kwok, J. W. Y. Lam, B. Z. Tang, *J. Am. Chem. Soc.* **2019**, *141*, 5612.
59. S. Liu, X. Zhou, H. Zhang, H. Ou, J. W. Y. Lam, Y. Liu, L. Shi, D. Ding, B. Z. Tang, *J. Am. Chem. Soc.* **2019**, *141*, 5359.
60. F. Hu, S. D. Xu, B. Liu, *Adv. Mater.* **2018**, *30*, 1801350.
61. Y. Liu, B. Liu, Z. Nie, *Nano Today* **2015**, *10*, 278.
62. F. Xia, J. Wu, X. Wu, Q. Y. Hu, J. Dai, X. D. Lou, *Acc. Chem. Res.* **2019**, *52*, 3064.
63. S. Xu, Y. Duan, B. Liu, *Adv. Mater.* **2020**, *32*, 1903530.
64. D. Y. Yan, Q. Wu, D. Wang, B. Z. Tang, *Angew. Chem. Int. Ed.* **2021**, *60*, 15724.
65. J. M. Zayed, N. Nouvel, U. Rauwald, O. A. Scherman, *Chem. Soc. Rev.* **2010**, *39*, 2806.
66. A. Kakkar, G. Traverso, O. C. Farokhzad, R. Weissleder, R. Langer, *Nat. Rev. Chem.* **2017**, *1*, 0063.
67. A. P. Blum, J. K. Kammeyer, A. M. Rush, C. E. Callmann, M. E. Hahn, N. C. Gianneschi, *J. Am. Chem. Soc.* **2015**, *137*, 2140.
68. S. Wang, P. Huang, X. Chen, *ACS Nano* **2016**, *10*, 2991.
69. J.-J. Hu, W. Jiang, L. Yuan, C. Duan, Q. Yuan, Z. Long, X. Lou, F. Xia, *Aggregate* **2021**, *2*, 48.
70. Y. Altay, S. Cao, H. Che, L. K. E. A. Abdelmohsen, J. C. M. van Hest, *Biomacromolecules* **2019**, *20*, 4053.
71. Y. Wang, J. Nie, W. Fang, L. Yang, Q. Hu, Z. Wang, J. Z. Sun, B. Z. Tang, *Chem. Rev.* **2020**, *120*, 4534.
72. Y. Liu, Y. Zhang, Z. Wang, J. Wang, K. Wei, G. Chen, M. Jiang, *J. Am. Chem. Soc.* **2016**, *138*, 12387.
73. W. Qi, Y. Zhang, J. Wang, G. Tao, L. Wu, Z. Kochovski, H. Gao, G. Chen, M. Jiang, *J. Am. Chem. Soc.* **2018**, *140*, 8851.
74. H. Schlaad, L. You, R. Sigel, B. Smarsly, M. Heydenreich, A. Mantion, A. Mašić, *Chem. Comm.* **2009**, 1478.
75. M. Liu, P. Gao, Q. Wan, F. Deng, Y. Wei, X. Zhang, *Macromol. Rapid Commun.* **2017**, *38*, 1600575.
76. Z. Wang, S. Chen, J. W. Y. Lam, W. Qin, R. T. K. Kwok, N. Xie, Q. Hu, B. Z. Tang, *J. Am. Chem. Soc.* **2013**, *135*, 8238.
77. B. Wang, P. Chen, J. Zhang, X.-C. Chen, Y.-H. Liu, Z. Huang, Q.-Y. Yu, J.-H. Zhang, W. Zhang, X. Wei, X.-Q. Yu, *Poly. Chem.* **2017**, *8*, 7486.
78. K. Yan, S. Zhang, K. Zhang, Y. Miao, Y. Qiu, P. Zhang, X. Jia, X. Zhao, *Poly. Chem.* **2020**, *11*, 7704.
79. M. Wang, L. Xu, M. Lin, Z. Li, J. Sun, *Poly. Chem.* **2021**, *12*, 2825.
80. H. Wang, G. Liu, S. Dong, J. Xiong, Z. Du, X. Cheng, *J. Mater. Chem. B* **2015**, *3*, 7401.
81. Y. Chen, H. Han, H. Tong, T. Chen, H. Wang, J. Ji, Q. Jin, *ACS Appl. Mater. Interfaces* **2016**, *8*, 21185.
82. L. Tang, J. K. Jin, A. Qin, W. Zhang Yuan, Y. Mao, J. Mei, J. Zhi Sun, B. Zhong Tang, *Chem. Comm.* **2009**, *45*, 4974.
83. P. Wu, X. Wang, Z. Wang, W. Ma, J. Guo, J. Chen, Z. Yu, J. Li, D. Zhou, *ACS Appl. Mater. Interfaces* **2019**, *11*, 18691.
84. R. Cheng, F. Meng, C. Deng, Z. Zhong, *Nano Today* **2015**, *10*, 656.
85. V. P. Torchilin, *Nat. Rev. Drug Discov.* **2014**, *13*, 813.
86. S. Mura, J. Nicolas, P. Couvreur, *Nat. Mater.* **2013**, *12*, 991.
87. D. J. Yang, S. Gao, Y. Fang, X. J. Lin, X. C. Jin, X. Y. Wang, L. Y. Ke, K. Shi, *Nanomedicine* **2018**, *13*, 3159.
88. Y. Yuan, S. Xu, C.-J. Zhang, B. Liu, *Poly. Chem.* **2016**, *7*, 3530.
89. M. S. Messina, K. M. M. Messina, A. Bhattacharya, H. R. Montgomery, H. D. Maynard, *Prog. Polym. Sci.* **2020**, *100*, 101186.
90. D. J. Siegwart, J. K. Oh, K. Matyjaszewski, *Prog. Polym. Sci.* **2012**, *37*, 18.
91. A. E. Smith, X. Xu, C. L. McCormick, *Prog. Polym. Sci.* **2010**, *35*, 45.
92. G. Becker, F. R. Wurm, *Chem. Soc. Rev.* **2018**, *47*, 7739.
93. L. Mespouille, O. Coulembier, M. Kawalec, A. P. Dove, P. Dubois, *Prog. Polym. Sci.* **2014**, *39*, 1144.
94. X. Zhang, X. Zhang, B. Yang, M. Liu, W. Liu, Y. Chen, Y. Wei, *Poly. Chem.* **2014**, *5*, 399.
95. X. Zhang, X. Zhang, B. Yang, M. Liu, W. Liu, Y. Chen, Y. Wei, *Poly. Chem.* **2014**, *5*, 356.
96. Y. Zhao, W. Zhu, L. Ren, K. Zhang, *Poly. Chem.* **2016**, *7*, 5386.
97. G. Xie, C. Ma, X. Zhang, H. Liu, X. Guo, L. Yang, Y. Li, K. Wang, Y. Wei, *Colloids Surfaces. B* **2017**, *157*, 166.
98. B. Yang, X. Zhang, X. Zhang, Z. Huang, Y. Wei, L. Tao, *Mater. Today* **2016**, *19*, 284.
99. E. Blanco, H. Shen, M. Ferrari, *Nat. Biotechnol.* **2015**, *33*, 941.
100. Q. Sun, X. Sun, X. Ma, Z. Zhou, E. Jin, B. Zhang, Y. Shen, E. A. Van Kirk, W. J. Murdoch, J. R. Lott, T. P. Lodge, M. Radosz, Y. Zhao, *Adv. Mater.* **2014**, *26*, 7615.
101. F. Ahmed, R. I. Pakunlu, A. Brannan, F. Bates, T. Minko, D. E. Discher, *J. Control. Release* **2006**, *116*, 150.
102. F. Meng, G. H. M. Engbers, J. Feijen, *J. Control. Release* **2005**, *101*, 187.
103. C. Deng, Y. Jiang, R. Cheng, F. Meng, Z. Zhong, *Nano Today* **2012**, *7*, 467.
104. M. Elsabahy, K. L. Wooley, *Chem. Soc. Rev.* **2012**, *41*, 2545.
105. C. D. Spicer, C. Jumeaux, B. Gupta, M. M. Stevens, *Chem. Soc. Rev.* **2018**, *47*, 3574.
106. X. Tao, H. Chen, S. Trépout, J. Cen, J. Ling, M.-H. Li, *Chem. Comm.* **2019**, *55*, 13530.
107. W. Chen, F. Meng, R. Cheng, C. Deng, J. Feijen, Z. Zhong, *J. Control. Release* **2014**, *190*, 398.
108. J. Feng, R.-X. Zhuo, X.-Z. Zhang, *Prog. Polym. Sci.* **2012**, *37*, 211.
109. K. Fukushima, *Biomater. Sci.* **2016**, *4*, 9.
110. A. Das, P. Theato, *Chem. Rev.* **2016**, *116*, 1434.
111. H. Tian, Z. Tang, X. Zhuang, X. Chen, X. Jing, *Prog. Polym. Sci.* **2012**, *37*, 237.
112. S. Tempelaar, L. Mespouille, O. Coulembier, P. Dubois, A. P. Dove, *Chem. Soc. Rev.* **2013**, *42*, 1312.
113. S. Cao, J. Shao, Y. Xia, H. Che, Z. Zhong, F. Meng, J. C. M. van Hest, L. K. E. A. Abdelmohsen, D. S. Williams, *Small* **2019**, *15*, 1901849.
114. L. M. P. E. van Oppen, L. K. E. A. Abdelmohsen, S. E. van Emst-de Vries, P. L. W. Welzen, D. A. Wilson, J. A. M. Smeitink, W. J. H. Koopman, R. Brock, P. H. G. M. Willems, D. S. Williams, J. C. M. van Hest, *ACS Cent. Sci.* **2018**, *4*, 917.
115. N. Zhang, H. Chen, Y. Fan, L. Zhou, S. Trépout, J. Guo, M.-H. Li, *ACS Nano* **2018**, *12*, 4025.
116. S. Cao, J. Shao, H. Wu, S. Song, M. T. De Martino, I. A. B. Pijpers, H. Friedrich, L. K. E. A. Abdelmohsen, D. S. Williams, J. C. M. van Hest, *Nat. Commun.* **2021**, *12*, 2077.
117. S. Cao, Y. Xia, J. Shao, B. Guo, Y. Dong, I. A. B. Pijpers, Z. Zhong, F. Meng, L. K. E. A. Abdelmohsen, D. S. Williams, J. C. M. van Hest, *Angew. Chem. Int. Ed.* **2021**, *60*, 17629.
118. K. Yang, Y. Chang, J. Wen, Y. Lu, Y. Pei, S. Cao, F. Wang, Z. Pei, *Chem. Mater.* **2016**, *28*, 1990.
119. M. Hao, G. Sun, M. Zuo, Z. Xu, Y. Chen, X.-Y. Hu, L. Wang, *Angew. Chem. Int. Ed.* **2020**, *59*, 10095.
120. S. Guo, Y. Song, Y. He, X.-Y. Hu, L. Wang, *Angew. Chem. Int. Ed.* **2018**, *57*, 3163.
121. X.-M. Chen, Q. Cao, H. K. Bisoyi, M. Wang, H. Yang, Q. Li, *Angew. Chem. Int. Ed.* **2020**, *59*, 10493.
122. G. Yu, R. Zhao, D. Wu, F. Zhang, L. Shao, J. Zhou, J. Yang, G. Tang, X. Chen, F. Huang, *Poly. Chem.* **2016**, *7*, 6178.
123. H. Huang, D. Xu, M. Liu, R. Jiang, L. Mao, Q. Huang, Q. Wan, Y. Wen, X. Zhang, Y. Wei, *Mater. Sci. Eng. C* **2017**, *78*, 862.
124. H. C. Zhang, Z. N. Liu, Y. L. Zhao, *Chem. Soc. Rev.* **2018**, *47*, 5491.
125. Z. Liu, X. Dai, Y. Sun, Y. Liu, *Aggregate* **2020**, *1*, 31.
126. J. Zhou, L. Rao, G. C. Yu, T. R. Cook, X. Y. Chen, F. H. Huang, *Chem. Soc. Rev.* **2021**, *50*, 2839.
127. D. Y. Xia, P. Wang, X. F. Ji, N. M. Khashab, J. L. Sessler, F. H. Huang, *Chem. Rev.* **2020**, *120*, 6070.
128. G. C. Yu, K. C. Jie, F. H. Huang, *Chem. Rev.* **2015**, *115*, 7240.
129. B. Qin, Z. H. Yin, X. Y. Tang, S. Zhang, Y. H. Wu, J. F. Xu, X. Zhang, *Prog. Polym. Sci.* **2020**, *100*, 101167.
130. L. L. Yang, X. X. Tan, Z. Q. Wang, X. Zhang, *Chem. Rev.* **2015**, *115*, 7196.

131. X. Chi, H. Zhang, G. I. Vargas-Zúñiga, G. M. Peters, J. L. Sessler, *J. Am. Chem. Soc.* **2016**, *138*, 5829.
132. D. Wu, Y. Li, J. Yang, J. Shen, J. Zhou, Q. Hu, G. Yu, G. Tang, X. Chen, *ACS Appl. Mater. Interfaces* **2017**, *9*, 44392.
133. X. Ji, Y. Li, H. Wang, R. Zhao, G. Tang, F. Huang, *Poly. Chem.* **2015**, *6*, 5021.
134. H. Cabral, K. Miyata, K. Osada, K. Kataoka, *Chem. Rev.* **2018**, *118*, 6844.
135. D. Li, Z. Tang, Y. Gao, H. Sun, S. Zhou, *Adv. Funct. Mater.* **2016**, *26*, 66.
136. F. Meng, C. Hiemstra, G. H. M. Engbers, J. Feijen, *Macromolecules* **2003**, *36*, 3004.
137. A. Hanisch, A. H. Gröschel, M. Förtsch, M. Drechsler, H. Jinnai, T. M. Ruhland, F. H. Schacher, A. H. E. Müller, *ACS Nano* **2013**, *7*, 4030.
138. S. Ha, Y. La, K. T. Kim, *Acc. Chem. Res.* **2020**, *53*, 620.
139. C. K. Wong, M. H. Stenzel, P. Thordarson, *Chem. Soc. Rev.* **2019**, *48*, 4019.
140. S. Cao, L. K. E. A. Abdelmohsen, J. Shao, J. van den Dikkenberg, E. Mastrobattista, D. S. Williams, J. C. M. van Hest, *ACS Macro Lett*. **2018**, *7*, 1394.
141. X. Jiang, W. Qu, D. Pan, Y. Ren, J.-M. Williford, H. Cui, E. Luijten, H.-Q. Mao, *Adv. Mater.* **2013**, *25*, 227.
142. J.-M. Williford, J. L. Santos, R. Shyam, H.-Q. Mao, *Biomater. Sci.* **2015**, *3*, 894.
143. I. A. B. Pijpers, L. K. E. A. Abdelmohsen, Y. Xia, S. Cao, D. S. Williams, F. Meng, J. C. M. van Hest, Z. Zhong, *Adv. Ther.* **2018**, *1*, 1800068.
144. D. S. Williams, I. A. B. Pijpers, R. Ridolfo, J. C. M. van Hest, *J. Control. Release* **2017**, *259*, 29.
145. A. Qin, J. W. Y. Lam, B. Z. Tang, *Prog. Polym. Sci.* **2012**, *37*, 182.
146. H. Chen, Y. Fan, N. Zhang, S. Trépout, B. Ptissam, A. Brûlet, B. Z. Tang, M.-H. Li, *Chem. Sci.* **2021**, *12*, 5495.
147. H. Chen, E. Zhang, G. Yang, L. Li, L. Wu, Y. Zhang, Y. Liu, G. Chen, M. Jiang, *ACS Macro Lett*. **2019**, *8*, 893.
148. H. Chen, Y. Fan, X. Yu, V. Semetey, S. Trépout, M.-H. Li, *ACS Nano* **2021**, *15*, 884.
149. M. Huo, Q. Ye, H. Che, X. Wang, Y. Wei, J. Yuan, *Macromolecules* **2017**, *50*, 1126.
150. D. Zhang, Y. Fan, H. Chen, S. Trépout, M.-H. Li, *Angew. Chem. Int. Ed.* **2019**, *58*, 10260.
151. X. L. Cai, B. Liu, *Angew. Chem. Int. Ed.* **2020**, *59*, 9868.
152. L. Yan, Y. Zhang, B. Xu, W. Tian, *Nanoscale* **2016**, *8*, 2471.
153. H. Cao, Y. Yang, J. Li, *Aggregate* **2020**, *1*, 69.
154. Z. Qiu, X. Liu, J. W. Y. Lam, B. Z. Tang, *Macromol. Rapid Commun.* **2019**, *40*, 1800568.
155. T. Han, L. Liu, D. Wang, J. Yang, B. Z. Tang, *Macromol. Rapid Commun.* **2021**, *42*, 2000311.
156. R. Hu, X. Yang, A. Qin, B. Z. Tang, *Mater. Chem. Front.* **2021**, *5*, 4073.
157. J. Chen, X. Chen, Q. Huang, W. Li, Q. Yu, L. Zhu, T. Zhu, S. Liu, Z. Chi, *ACS Appl. Mater. Interfaces* **2019**, *11*, 32689.
158. Y. Li, R. T. K. Kwok, B. Z. Tang, B. Liu, *RSC Advances* **2013**, *3*, 10135.
159. B. Wang, C. Li, L. Yang, C. Zhang, L.-J. Liu, S. Zhu, Y. Chen, Y. Wang, *J. Mater. Chem. B* **2019**, *7*, 3846.
160. Z. Huang, Q. Chen, Q. Wan, K. Wang, J. Yuan, X. Zhang, L. Tao, Y. Wei, *Poly. Chem.* **2017**, *8*, 4805.
161. Z. Long, M. Liu, L. Mao, G. Zeng, Q. Wan, D. Xu, F. Deng, H. Huang, X. Zhang, Y. Wei, *Colloids Surfaces. B* **2017**, *150*, 114.
162. N. U. Deshpande, M. Virmani, M. Jayakannan, *Poly. Chem.* **2021**, *12*, 1549.
163. S. Saxena, M. Jayakannan, *Biomacromolecules* **2020**, *21*, 171.
164. Y. Li, X. Wu, B. Yang, X. Zhang, H. Li, A. Umar, N. F. d. Rooij, G. Zhou, Y. Wang, *ACS Appl. Mater. Interfaces* **2019**, *11*, 37077.
165. C. G. Palivan, R. Goers, A. Najer, X. Zhang, A. Car, W. Meier, *Chem. Soc. Rev.* **2016**, *45*, 377.
166. E. Rideau, R. Dimova, P. Schwille, F. R. Wurm, K. Landfester, *Chem. Soc. Rev.* **2018**, *47*, 8572.
167. X. Yi, J. Dai, Y. Han, M. Xu, X. Zhang, S. Zhen, Z. Zhao, X. Lou, F. Xia, *Commun. Biol.* **2018**, *1*, 202.
168. C. Sun, J. Lu, J. Wang, P. Hao, C. Li, L. Qi, L. Yang, B. He, Z. Zhong, N. Hao, *J Nanobiotechnol* **2021**, *19*, 14.
169. Q. Wang, F. Gao, X. Zhou, *Colloid Polym. Sci* **2020**, *298*, 1119.
170. C. Zhang, S. Jin, S. Li, X. Xue, J. Liu, Y. Huang, Y. Jiang, W.-Q. Chen, G. Zou, X.-J. Liang, *ACS Appl. Mater. Interfaces* **2014**, *6*, 5212.
171. Y. Yuan, C.-J. Zhang, B. Liu, *Angew. Chem. Int. Ed.* **2015**, *54*, 11419.
172. H. Wang, G. Liu, H. Gao, Y. Wang, *Poly. Chem.* **2015**, *6*, 4715.
173. Y. Dai, C. Xu, X. Sun, X. Chen, *Chem. Soc. Rev.* **2017**, *46*, 3830.
174. W. Zhuang, B. Ma, J. Hu, J. Jiang, G. Li, L. Yang, Y. Wang, *Theranostics* **2019**, *9*, 6618.
175. G. Yu, M. Zhang, M. L. Saha, Z. Mao, J. Chen, Y. Yao, Z. Zhou, Y. Liu, C. Gao, F. Huang, X. Chen, P. J. Stang, *J. Am. Chem. Soc.* **2017**, *139*, 15940.
176. X. W. He, L. H. Xiong, Z. Zhao, Z. Y. Wang, L. Luo, J. W. Y. Lan, R. T. K. Kwok, B. Z. Tang, *Theranostics* **2019**, *9*, 3223.
177. D. Wang, M. M. S. Lee, W. H. Xu, R. T. K. Kwok, J. W. Y. Lam, B. Z. Tang, *Theranostics* **2018**, *8*, 4925.
178. M. Kang, Z. Zhang, N. Song, M. Li, P. Sun, X. Chen, D. Wang, B. Z. Tang, *Aggregate* **2020**, *1*, 80.
179. G. Qi, F. Hu, Kenry, K. C. Chong, M. Wu, Y. H. Gan, B. Liu, *Adv. Funct. Mater.* **2020**, *30*, 2070206.
180. M. Chen, J. He, S. Xie, T. Wang, P. Ran, Z. Zhang, X. Li, *J. Control. Release* **2020**, *322*, 326.
181. J. Li, I. Rozen, J. Wang, *ACS Nano* **2016**, *10*, 5619.
182. B. Esteban-Fernández de Ávila, P. Angsantikul, J. Li, W. Gao, L. Zhang, J. Wang, *Adv. Funct. Mater.* **2018**, *28*, 1705640.
183. K. K. Dey, A. Sen, *J. Am. Chem. Soc.* **2017**, *139*, 7666.
184. A. C. Hortelão, T. Patiño, A. Perez-Jiménez, À. Blanco, S. Sánchez, *Adv. Funct. Mater.* **2018**, *28*, 1705086.
185. L. K. E. A. Abdelmohsen, M. Nijemeisland, G. M. Pawar, G.-J. A. Janssen, R. J. M. Nolte, J. C. M. van Hest, D. A. Wilson, *ACS Nano* **2016**, *10*, 2652.
186. I. A. B. Pijpers, S. Cao, A. Llopis-Lorente, J. Zhu, S. Song, R. R. M. Joosten, F. Meng, H. Friedrich, D. S. Williams, S. Sánchez, J. C. M. van Hest, L. K. E. A. Abdelmohsen, *Nano Lett*. **2020**, *20*, 4472.
187. D. Xu, C. Zhou, C. Zhan, Y. Wang, Y. You, X. Pan, J. Jiao, R. Zhang, Z. Dong, W. Wang, X. Ma, *Adv. Funct. Mater.* **2019**, *29*, 1807727.
188. J. Shao, M. Abdelghani, G. Shen, S. Cao, D. S. Williams, J. C. M. van Hest, *ACS Nano* **2018**, *12*, 4877.
189. X. Xu, S. Hou, N. Wattanatorn, F. Wang, Q. Yang, C. Zhao, X. Yu, H.-R. Tseng, S. J. Jonas, P. S. Weiss, *ACS Nano* **2018**, *12*, 4503.
190. F. Zhang, J. Zhuang, B. Esteban Fernández de Ávila, S. Tang, Q. Zhang, R. H. Fang, L. Zhang, J. Wang, *ACS Nano* **2019**, *13*, 11996.
191. M. Hansen-Bruhn, B. E.-F. de Ávila, M. Beltrán-Gastélum, J. Zhao, D. E. Ramírez-Herrera, P. Angsantikul, K. Vesterager Gothelf, L. Zhang, J. Wang, *Angew. Chem. Int. Ed.* **2018**, *57*, 2657.
192. W. Wang, Z. Wu, X. Lin, T. Si, Q. He, *J. Am. Chem. Soc.* **2019**, *141*, 6601.
193. S. Tang, F. Zhang, H. Gong, F. Wei, J. Zhuang, E. Karshalev, B. Esteban-Fernández de Ávila, C. Huang, Z. Zhou, Z. Li, L. Yin, H. Dong, R. H. Fang, X. Zhang, L. Zhang, J. Wang, *Sci. Robot.* **2020**, *5*, eaba6137.
194. V. Magdanz, S. Sanchez, O. G. Schmidt, *Adv. Mater.* **2013**, *25*, 6581.
195. H. Wang, M. Pumera, *Chem. Rev.* **2015**, *115*, 8704.
196. T. Xu, W. Gao, L.-P. Xu, X. Zhang, S. Wang, *Adv. Mater.* **2017**, *29*, 1603250.
197. H. Wang, M. Pumera, *Adv. Funct. Mater.* **2018**, *28*, 1705421.
198. C. K. Schmidt, M. Medina-Sánchez, R. J. Edmondson, O. G. Schmidt, *Nat. Commun.* **2020**, *11*, 5618.
199. L. Xu, F. Mou, H. Gong, M. Luo, J. Guan, *Chem. Soc. Rev.* **2017**, *46*, 6905.
200. J. Wang, Z. Xiong, J. Zheng, X. Zhan, J. Tang, *Acc. Chem. Res.* **2018**, *51*, 1957.
201. M. J. Xuan, R. Mestre, C. Y. Gao, C. Zhou, Q. He, S. Sanchez, *Angew. Chem. Int. Ed.* **2018**, *57*, 6838.
202. J. Shao, S. Cao, D. S. Williams, L. K. E. A. Abdelmohsen, J. C. M. van Hest, *Angew. Chem. Int. Ed.* **2020**, *59*, 16918.
203. M. Xuan, Z. Wu, J. Shao, L. Dai, T. Si, Q. He, *J. Am. Chem. Soc*. **2016**, *138*, 6492.
204. M. Xuan, J. Shao, C. Gao, W. Wang, L. Dai, Q. He, *Angew. Chem. Int. Ed.* **2018**, *57*, 12463.
205. X. Ma, K. Hahn, S. Sanchez, *J. Am. Chem. Soc*. **2015**, *137*, 4976.
206. D. Xu, Y. Wang, C. Liang, Y. You, S. Sanchez, X. Ma, *Small* **2020**, *16*, 1902464.
207. A. C. Hortelao, C. Simó, M. Guix, S. Guallar-Garrido, E. Julián, D. Vilela, L. Rejc, P. Ramos-Cabrer, U. Cossío, V. Gómez-Vallejo, T. Patiño, J. Llop, S. Sánchez, *Sci. Robot.* **2021**, *6*, eabd2823.

208. A. C. Hortelão, R. Carrascosa, N. Murillo-Cremaes, T. Patiño, S. Sánchez, *ACS Nano* **2019**, *13*, 429.

AUTHOR BIOGRAPHIES

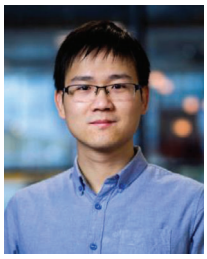

Shoupeng Cao obtained his PhD degree in 2020 at Eindhoven University Technology under the guidance of Prof. Dr. Jan C. M. van Hest. His thesis was focused on the engineering well-defined biodegradable polymeric nanoparticles towards tailored biomedical applications. Currently, he holds a post-doctoral position at the Max Planck Institute for Polymer Research under supervision of Prof. Dr. Katharina Landfester. His research interests include polymeric nanocompartments for biomedicine applications and biomimicry microcompartments with adaptive and life-like features.

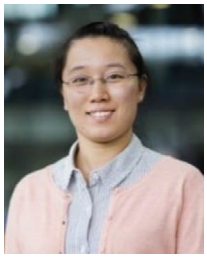

Jingxin Shao obtained her PhD degree in Chemical Engineering and Technology from Harbin Institute of Technology. As a visiting PhD student, she received the opportunity to work at the Institute of Chemistry, Chinese Academy of Sciences (ICCAS) and National Center for Nanoscience and Technology (NCNST). She then moved to Eindhoven University of Technology in The Netherlands for postdoctoral research in the Bio-Organic Chemistry research group headed by Prof. Dr. Jan van Hest. Her research interests include self-assembled supramolecular micro/nanoarchitectures, life-like artificial cells, bio-inspired micro/nanoswimmers and their application in biomedicine.

Loai Abdelmohsen is assistant professor in the institute for complex molecular systems (ICMS) at Eindhoven University of Technology. In 2017, he obtained his PhD degree in Chemistry at Radboud University. Loai's research lies within two interrelated areas: (1) The design of dynamic responsive colloidal mesosystems and (2) The development of active machinery (micro/nanomotors). He has been awarded the young researchers award from the Volkswagen foundation on his work in the field of Micro and Nanomachines. Loai is an expert in the characterization of nanoparticles using light scattering as a particle analysis technique that is critical and very useful for understanding the nature of nanoscale assemblies.

Jan van Hest obtained his PhD from Eindhoven University of Technology (TU/e) in 1996 with Prof. E.W. Meijer. In 2000, he was appointed full professor at Radboud University Nijmegen. As of September 2016 he holds the chair of Bio-organic Chemistry at TU/e. Since May 2017, he is the scientific director of the Institute for Complex Molecular Systems (ICMS). The group's focus is to develop well-defined compartments for nanomedicine and artificial cell research, using a combination of techniques from polymer science to protein engineering.

How to cite this article: S. Cao, J. Shao, L. K. E. A. Abdelmohsen, J. C. M. van Hest, *Aggregate* **2022**, *3*, e128. https://doi.org/10.1002/agt2.128